Assessment of the radiological risks and heavy metal pollution on the water quality of the Vaal River, South Africa

BT Chobeka

https://orcid.org/0000-0003-2010-0423

Thesis accepted in fulfilment of the requirements for the degree Doctor of Philosophy in Science Radiation Science at the North-West University

Promoter: Prof M Mathuthu

Graduation: July 2024

DECLARATION

I, Boitshekwane Tryphina Chobeka (Student number: 20941250), hereby declare that the work presented in this thesis is a product of my own research. It has not been submitted in part or whole for any degree at any other university before. The data presented is original, and the author did all analyses under the guidance of the supervisors. Any data taken from other sources has been referred to and fully acknowledged

Signature of the student:

Date: 18/07/2024

Boitshekwane T Chobeka

DEDICATION

This work is dedicated to my family for their encouragement and loving support during my Ph.D studies. I can never forget my caring husband, Dedrick Sinethemba Chobeka, my son Thato Kgantsi and my daughter Lukhanyo Chobeka, who tolerated my absence from home throughout my studies. Without their motivation and patience, my goals would not have been accomplished. I would also like to dedicate this work to my relatives and friends who have always been there for me when things appeared to be impossible. Lastly, I would like to pay special tribute to my late father, Ben Lekgolo Kgantsi, who was my main source of inspiration. May his soul rest in eternal peace.

Above all, my deepest gratitude goes to my Lord for the strength and wisdom He has given me throughout this project and to my pastor, Moses Kgantsi, and his wife, Rose Kgantsi, for their prayers and support.

ACKNOWLEDGEMENT

This research work was conducted at the North-West University (Mahikeng Campus) through the Centre for Applied Radiation Science and Technology (CARST). I would like to thank Prof. Manny Mathuthu, my Supervisor from North-West University, for providing an enabling and conducive environment and excellent support in my study, as well as Dr Atsile Ocwelwang, my co-supervisor, for providing outstanding assistance throughout my studies. Their valuable suggestions and thoughtful criticisms guided me and resulted in the completion of this thesis.

I would also like to thank the Faculty of Natural and Agricultural Science (FNAS) and the North-West University Bursary scheme for the financial support that made it possible to carry out my studies. My gratitude also goes to all the employees of CARST who helped me with the needed resources. Special attention goes to Ms Mokgele, the Senior Technician at CARST who worked tirelessly in many ways and assisted in procuring liquid nitrogen that was required for Gamma Spectroscopy.

Furthermore, I would like to extend my gratitude to Mr Moses Radebe for assuring that the samples were changed in due time for the Gamma Spectroscopy analysis and Dr ND Mokhine for ensuring that all my samples were well prepared and ready for ICP-MS. My heartfelt thanks also go to my fellow Ph.D student at CARST, OA Jegede, for outstanding and remarkable assistance as well as moral support throughout my study. Lastly, Dr Tebogo Kupi continually made sure that his door was always open to offer scientific advice throughout my studies.

ABSTRACT

Anthropogenic activities close to water bodies contribute to poor water quality, degrading the natural conditions of plants and animals and elevating health risks concerning humans. The Vaal River supplies potable water to the Gauteng, North West, Free State, Northern Cape, and Mpumalanga provinces of South Africa. Consequently, the water quality of the Vaal River needs to be monitored and assessed for radioactivity and heavy metal risks. The aim of this study was to investigate the concentration levels of NORM radionuclides and heavy metals and their effect on the water quality of the Vaal River. As a result, 27 water samples were collected and analysed for U, Th & K as well as toxic heavy metal concentrations that may potentially cause risks to the public around the study area, using the inductively coupled plasma mass spectroscopy (ICP-MS) technique. The risks of pollutant exposure of humans to heavy metals in water were evaluated using chronic daily intake (CDI), hazard quotient (HQ), and hazard index (HI), heavy metal pollution index (MPI) and heavy metal evaluation index (HEI). Ion chromatography (IC) was also used to examine water types from the cations and anions therein. The cations measured are calcium (Ca^{2+}), sodium (Na^{+}), magnesium (Mg^{2+}), and potassium (K^{+}). Anions measured were sulphate, phosphate, nitrite and reflected on a Piper diagram.

Results show that:

i. The activity concentrations of K, U and Th (Bq/l) were used to assess the radiological health indices by calculating the radium equivalent activity (Ra_{eq}), dose rate (D), annual effective dose (AEDE), external hazard (H_{ex}) and internal hazard (H_{in}). The calculated average radiation hazard index for Ra_{eq} was (33.803 Bq/l), D (18.158 nGy/hr), AEDE 0.0222 (nGy/hr), H_{ex} (0.091) and H_{in} (0,096) in this study. These hazard parameters were lower than the world average permissible limit. A a result, the water from the Vaal River does not pose radiological risks to members of the public.
ii. The HEI values for all heavy metals, like Li and Fe were less than 40, indicating low pollution level, while for Mn, HEI = 80.35. From the MPI & HEI values of Li, Fe & Mn, we conclude that Mn & Fe, are the major pollutant of the water in the Vaal River. This could be due to human activities such as discharges from nearby industries and mines. According to the findings of the study, the Vaal River is not suitable for use

(drinking or recreational) due to pollution by these two heavy metals emanating from nearby industries.

iii. Ion chromatography (IC) was used also to examine the cations and anions of the study. The cations: calcium (Ca^{2+}), sodium (Na^{+}), magnesium (Mg^{2+}), and potassium (K^{+}), had an average concentration of 34.4, 58.9, 13.8, and 6.3 mg/l, respectively. The anions: sulphate (SO_4^{2-}), phosphate (PO_4^{3-}), and nitrite (NO_2), had an average concentration of 87.5, 0.7, and 0.1 mg/l, respectively. The piper results indicated that the Vaal River is of a Ca-Mg-SO2 water type, with no dominating phase.

Based on the findings of the study, we concluded that there is no radiological risk from the Vaal River waters in the study area. However, the heavy metal concentrations in this study prove that the Vaal River is not safe for public use due to increased levels of Mn and Fe at 1.34 mg/l and 4.02 mg/l respectively across the river flow. As a result, additional river monitoring is required to maintain public safety. This study recommends a conceptual management plan to assist relevant stakeholders in the maintenance of the water quality for the Vaal River.

TABLE OF CONTENTS

List of figures

List of tables

List of abbreviations

BEGe	Broad Energy Germanium
ICP-MS	Inductively coupled plasma mass spectroscopy
MCA	Multi-channel analyser
NNR	National Nuclear Regulator
NORM	Naturally occurring radioactive material
WHO	World Health Organisation
WRC	Water Research Commission
DWS	Department of Water and Sanitation
DWA	Department of Water Affairs
SALGA	South African Local Government Association
UNSCEAR	United Nations Scientific Committee on the Effects of Atomic Radiation
GPS	Global positioning system
AEDE	Annual effective dose equivalent
Ra_{eq}	Radium equivalent activity
H_{ex}	External hazard index
K	Potassium
Th	Thorium
U	Uranium
mSv	Millisievert
Bq/kg	Becquerel per kilogram
CARST	Centre for Applied Radiation Science and Technology
nGy/hr	nano Gray per hour
HCl	hydrochloric acid
ppb	parts per billion
ppm	parts per million

CHAPTER 2: INTRODUCTION AND PROBLEM STATEMENT

1.1 Introduction

The issues of river water pollution by various anthropogenic activities in South Africa are of major concern (Claassens *et al.*, 2016, Zhou *et al.*, 2020b). Water pollution is the contamination of water bodies such as rivers or lakes by human activity, which has a negative impact on water users (Ajibade *et al.*, 2021). Toxins from sewage discharges, industrial operations, mining, agriculture, and urban or storm-water runoff interact with water bodies to cause contamination (Moloi *et al.*, 2020, Wolkersdorfer *et al.*, 2021). When humans use contaminated water for various activities such as drinking or irrigation, it can cause ecosystem destruction and spread water-borne diseases (Mararakanye *et al.*, 2022, Mokarram *et al.*, 2020, Moloi *et al.*, 2020). The more polluted water bodies there are, the worse the water quality becomes (Du Plessis, 2021). According to numerous studies, the main causes of South Africa's poor water quality are mining, urbanization, and other anthropogenic causes (Durand, 2012, Manyatshe *et al.*, 2017, Van Rensburg *et al.*, 2016, Winde *et al.*, 2017).

South Africa has many aspects of water challenges that can affect the country's economic growth, especially when the levels of water scarcity, droughts, as well as increasing and deteriorating water resources are not well addressed (Plessl *et al.*, 2019, Van Rensburg *et al.*, 2016, Wepener *et al.*, 2011). Potable water is essential to life. Therefore, it is important to ensure that its quality is maintained through careful monitoring activities (Du Plessis, 2021).

In addition, South Africa is known for its mining industry, which plays an important economic role (Winde *et al.*, 2017, Worlanyo and Jiangfeng, 2021). South Africa is also considered the largest gold producer in the world (Winde and de Villiers, 2002). The Gauteng province within the Witwatersrand Basin of South Africa, has more uranium than gold, which was mined as a by-product. Mining of uranium within the Gauteng province is mainly on the outskirts of Johannesburg, near Randfontein, and west of the Witwatersrand (Winde and de Villiers, 2002). Uranium waste recovered from the gold mining operations is deposited in the Witwatersrand mud dams. Over the years, the waste piles grew and increased radionuclides levels in the environment (Winde *et al.*, 2017, Worlanyo and Jiangfeng, 2021).

According to Du Plessis (2021), the sustainability of South Africa's freshwater resources is at a critical point. The South African water bodies need the attention and status they deserve to

ensure that the quality of water is in the desired state for users (Makubalo and Diamond, 2020). Within Gauteng and the North West Province of South Africa, the deterioration of rivers due to mining activities is noticeable (Durand, 2012). Mines are allegedly the major environmental sources of radionuclides and heavy metals (Durand, 2012, Manyatshe *et al.*, 2017, Van Rensburg *et al.*, 2016, Winde *et al.*, 2017).

Radionuclides and heavy metals are normally released during surface mining operations (Manyatshe *et al.*, 2017, Van Rensburg *et al.*, 2016, Winde *et al.*, 2017). They are found naturally everywhere in the environment and can accumulate easily in soil and water (Manyatshe *et al.*, 2017, Van Rensburg *et al.*, 2016, Winde *et al.*, 2017). The concentration of radioactive materials and heavy metals produced during mining processes can potentially cause serious risks to people and the environment when exposed to persistent levels (Groffen *et al.*, 2018, Marara and Palamuleni, 2019, Moloi *et al.*, 2020).

Furthermore, mines are considered liable for a series of environmental issues and human health problems (Plessl *et al.*, 2019, Van Rensburg *et al.*, 2016, Wepener *et al.*, 2011) and can potentially cause severe risks to the environment and people (Plessl *et al.*, 2019, Van Rensburg *et al.*, 2016). Some of these risks include damage to water bodies, biodiversity loss, and changes in lifestyle, as well as affecting food security and potentially causing pollution (Plessl *et al.*, 2019, Van Rensburg *et al.*, 2016). The risks can be due to the decay series of the long-lived natural radionuclides of uranium (U) and thorium (Th) (Madzunya *et al.*, 2020). The radionuclides can enter the environment and cause various health effects when ingested or inhaled in high concentrations, resulting in illnesses such as cancer and eye problems (Davies and Mundalamo, 2010).

According to Durand (2012), the Gauteng and North West mine effluent contains thorium, uranium, radium and polonium, which are considered radioactive. These pollutants accumulate in the river sediments and the soil, posing a severe effect on the water, the environment and the people (Durand, 2012). Exposure to these pollutants may potentially cause destruction of the kidneys, blindness, paralysis, cancer, tissue disease and changes in the immune system (Durand, 2012, Jibiri and Okeyode, 2012, Moloi *et al.*, 2020). The permissible limit of uranium in drinking water is 30 mg/l, as per the recommendation by the World Health Organization (WHO) (Burritt and Christ, 2018). The level is based on the epidemiology studies of consumption of 2 litre of drinking water by a 70 kg adult per day, with an 80% tolerable daily intake (Ma *et al.*, 2020).

1.2 Problem Statement

Rivers provide needed potable water for agricultural activities, industrial, mining and domestic purposes. Rivers supply water to many urban areas. During dry seasons, river water is used to supplement rainfall, ensuring sustained crop production (Du Plessis, 2021). In this study, the Vaal River provides needed potable water to varied industries in the Gauteng, North West, Northern Cape, Free State and Mpumalanga provinces of South Africa (Davies and Mundalamo, 2010, Durand, 2012, Manyatshe *et al.*, 2017). However, these same industries tend to discharge polluted water back into the river system and degrade the water quality of the river (Atangana and Oberholster, 2021, Marara and Palamuleni, 2019, Moloi *et al.*, 2020).

The Vaal River flows through gold mines and is potentially contaminated with substantial amounts of radionuclides and heavy metals (Manyatshe *et al.*, 2017). Furthermore, the Vaal River is argued to be a dumping site for radiotoxic and heavy metals from various industries, including mines (Durand, 2012). The state of the river shows no sign of improvement (Chokwe and Okonkwo, 2019, Wepener *et al.*, 2011). In 2017, Manyatshe *et al.* (2017) depicted high concentrations of NO_3 anion and declared the river water unfit for domestic and agricultural use. Heavy metal pollution such as zinc (Zn), arsenic (As), nickel (Ni) and uranium (U) were observed in 2019 by Marara and Palamuleni (2019). A year later, Moloi *et al.* (2020) projected health risks to humans due to high concentrations of arsenic, while Madzunya *et al.* (2020) projected high concentrations of ^{226}Ra. At this level, continued pollution of the river will potentially have serious impacts on human health, food production and the environment (Chokwe and Okonkwo, 2019, Van Rensburg *et al.*, 2016, Wepener *et al.*, 2011).

There are numerous studies conducted concerning the Vaal River water system and its pressing problems (Moloi *et al.*, 2020, Marara and Palamuleni, 2019, Manyatshe *et al.*, 2017). However, progress has not been made in addressing issues relating to the pollution of the river (Du Plessis, 2021, Van Rensburg *et al.*, 2019, Weideman *et al.*, 2020). Furthermore, not many studies concerning the radionuclides and heavy metals in the Vaal River have been conducted. Recent studies conducted around the Vaal River have been about the radioactivity levels and dosages of the mine dam tailings as well as the exposure of uranium to people (Moshupya, 2022, Zupunski *et al.*, 2023).

This study area was selected based on several pollution concerns from varied studies of the Vaal River (Chokwe *et al.*, 2017, Moloi *et al.*, 2020) and it focuses on the river as a possible

pathway for heavy metals and radionuclides intake. The aim is to assess the water quality of the river for future reference. The study looks at possible angles that may contribute to river water pollution, which affects the water quality of the river, and proposes a conceptual management model for the Vaal River.

Furthermore, it is significant to note that many South African gold mines extracting ore contain not only gold but a substantial amount of uranium (U), which is also transported to the surface inadvertently (Winde and de Villiers, 2002). The main problem of mining uranium is the widespread effects it brings to the environment, such as increased levels of radiation and water-borne toxins (Madzunya *et al*., 2020).

1.3 Previous studies

Previous studies have included assessment of radioactive elements in water by the National Nuclear Regulator (NNR) and Water Research Commission (WRC) of South Africa. The study by the WRC was conducted in 2010 while that of the NNR was in 2014. The NNR is mandated to regulate and prevent nuclear radioactive incidents affecting the environment and people, among other duties. The WRC mandate is to identify gaps in relation to areas of research for water. The study by Marara and Palamuleni (2019) on heavy metals is also examined in this study.

The NNR investigated the radiological effect of mining activity discharges in water and confirmed uranium as a toxic chemical (NNR, 2007). According to NNR's investigation, uranium affects the water catchment and poses risks to the surrounding communities. The WRC reported uranium concentrations in their scientific research report written in April 2010. The report investigated the concentration of uranium elements in the South African water catchments. According to the WRC, the concentration of uranium in the majority of the water catchments was above the 250 mSv/yr recommended limit regulated by the NNR (NNR, 2007). Furthermore, the study by Marara and Palamuleni (2019) on the water quality of the Klip River in Gauteng Province detected high concentrations of heavy metals. The Klip River is a tributary to the Vaal River. A recent study about the radioactivity level nearby the Gauteng gold mine tailing dams depicted high concentrations of U in the soil (Kamunda, 2017, Moshupya, 2022). Concerning heavy metals, Kamunda *et al* (2017) observed high concentrations of Ni and Zn in soil.

1.4 Justification

A lot of studies have been conducted concerning the Vaal River. However, not much has been done on the water quality of the river. (Groffen et al., 2018, Saad et al., 2022). Majority of the studies have been investigating the amount of waste pollution discarded into the river (Manyatshe et al., 2017, Saad et al., 2022). Less has been conducted on the toxic elements of the river (Marara and Palamuleni, 2019, Moloi et al., 2020). The objective of this study is to create awareness among the communities living around the Vaal River vicinity. The awareness is mainly based on the risks associated with high levels of heavy metals and radionuclides in the river. The reported results of the study are intended to improve risk assessment in relation to heavy metals and radionuclides through direct and indirect exposure of humans to these chemicals. The result of this study can also be used as the baseline database for water research materials. The findings of the study will be further used to provide a conceptual management plan for further planning and better management of the Vaal River. In short, this study will also be beneficial to several departments, such as Rand Water, the local municipality of the Vaal River and the community at large, through better management of the river as suggested by the study.

1.5 Aim and objectives of the study

1.5.1 Aim

The aim of this study was to investigate the concentration levels of the radionuclides and heavy metals and their effect on the water quality of the Vaal River.

1.5.2 Objectives

The objectives of this study were to:

- Assess the water quality of the Vaal River in terms of the NORM radionuclides.
- Determine the water quality of the Vaal River in terms of the heavy metal pollutants.
- Evaluate the radiological health risk indices due to NORM.
- Determine the risks associated with toxic heavy metals in water.
- Review the challenges and the sustainability of the Vaal River for future water supply to the North West and Gauteng Provinces.

- Propose a Conceptual Management model for sustainable water quality of the Vaal River.

1.6 Thesis outline

This study has five chapters. The first chapter is an introduction and provides a brief background on the radiological and heavy metal levels of the Vaal River. The chapter also highlights the relevance of the study and, the aim and objectives thereof. Chapter 2 is a review of literature on the following topics: potential pathways of heavy metal inputs, heavy metals in the river, the effects of heavy metals, and instruments used for analysis such as Inductively Coupled Plasma Mass Spectrometry (ICP-MS) and Ion Chromatography. The chapter further reviews the main radionuclides and the properties of naturally occurring radionuclides (NORMs). Chapter 3 describes the study area, the techniques used for data collection and preparation for laboratory analysis, the instruments used for data analysis, and the calculations used to measure the radiological risks, elemental risks and water quality. Chapter 4 presents, interprets and discuss the results of the study. Finally, the fifth chapter contains the conclusions and provides recommendations for future research in the identified gaps for better planning, maintenance and monitoring of the Vaal River.

CHAPTER 3: LITERATURE REVIEW

2.1 Introduction

Water quality refers to the state of the water, including its chemical, physical, and biological qualities, as well as its suitability for a certain purpose such as drinking or swimming (WHO, 2022). There are four sorts of water quality: drinkable water, appetizing water, contaminated (polluted) water, and infected water (Ajibade *et al.*, 2021). Contaminated water can cause major health issues, which can lead to serious sickness (Mokarram *et al.*, 2020, Rani *et al.*, 2022). Our rivers, reservoirs, lakes, and oceans are being polluted by chemicals, garbage, plastic, and other contaminants beyond control (Wepener *et al.*, 2011, Zhou *et al.*, 2020a).

The challenges of rising water consumption as a result of numerous human activities, such as mining in South Africa, are of great concern (Claassens *et al.*, 2016, Winde *et al.*, 2017). Rivers become severely contaminated due to the amount of garbage dumped into them (Tomno *et al.*, 2020). According to numerous studies, South Africa's poor water quality is largely caused by mining, urbanization, and other anthropogenic factors (Durand, 2012, Manyatshe *et al.*, 2017, Winde *et al.*, 2017). Given the water problems South Africa is dealing with, it is important to emphasize that if the country's economic development is not successfully addressed, the issue could have a negative impact (Rani *et al.*, 2022). Potable water is vital to life, hence, it is important to maintain its quality through monitoring programmes (Du Plessis, 2021).

In general, mines are argued to be the primary source of hazardous radionuclides such as uranium in waterways (Durand, 2012, Manyatshe *et al.*, 2017, Van Rensburg *et al.*, 2019, Winde *et al.*, 2017). These radionuclides provide a problem in that they can quickly assemble in the waterways (Durand, 2012, Manyatshe *et al.*, 2017, Van Rensburg *et al.*, 2019, Winde *et al.*, 2017). When exposed, people and the environment may face substantial dangers from high concentrations of hazardous radionuclides (Groffen *et al.*, 2018, Marara and Palamuleni, 2019, Moloi *et al.*, 2020). The long-lived natural radionuclide decay sequence of elements such as uranium (U) and thorium (Th) is what causes the dangers (Madzunya *et al.*, 2020). Figure 2.1 shows the decay series of Uand Th, to the daughter isotopes.

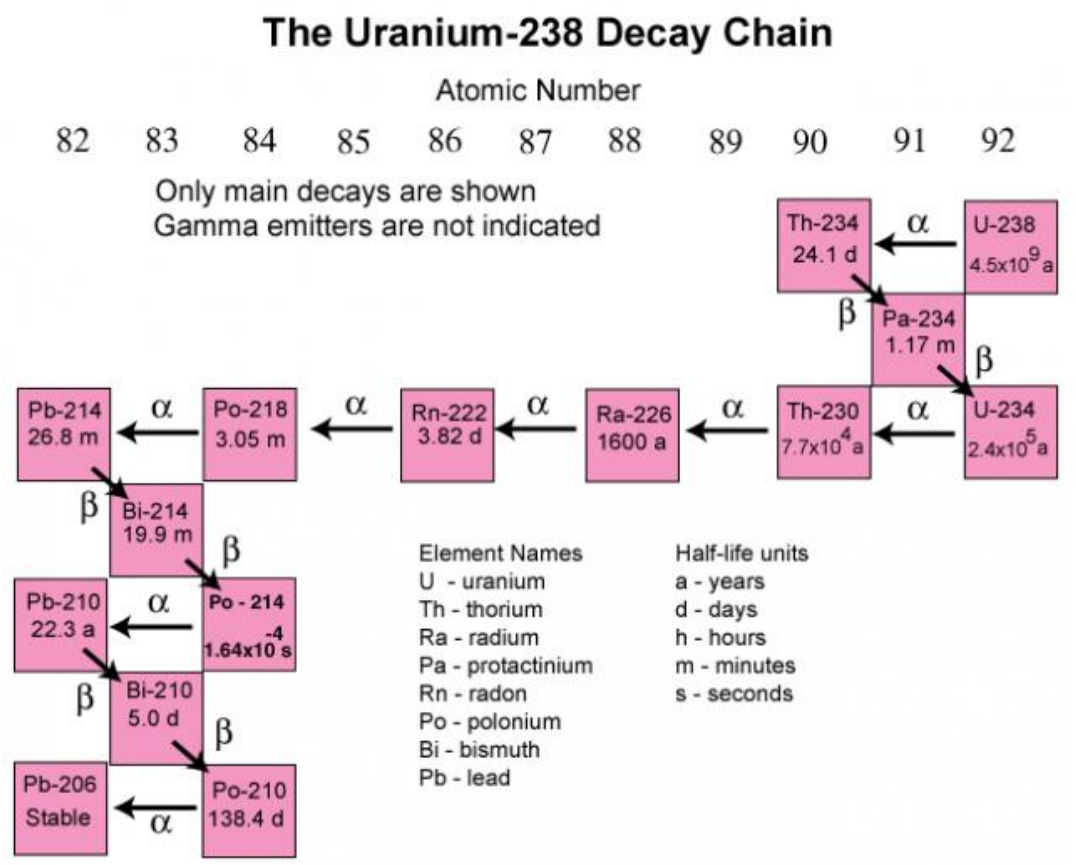

Figure 2. 1a: U decay series (Rutgers van der Loeff, 2019).

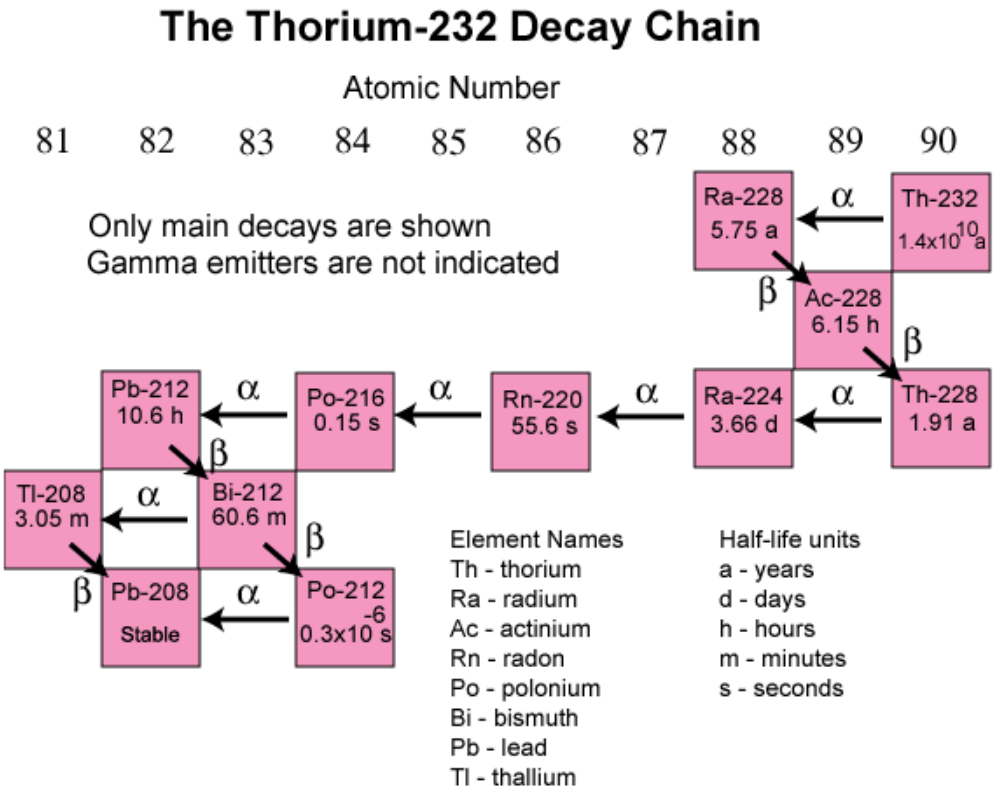

Figure 2. 2*b*: U decay series (Rutgers van der Loeff, 2019)

When U decays, it goes through a series of decay steps beginning with ^{238}U and ending with ^{206}Pb which is a stable isotope (Pourcelot *et al.*, 2021). The parent isotope ^{238}U decays into the daughter isotopes ^{234}U ^{230}Th and ^{226}Ra. The half- lives of the parent nuclide ^{238}U decay chain are substantially longer than those of the other intermediate nuclides such as ^{230}Th (Postar, 2017, Pourcelot *et al.*, 2021). The same applies when ^{232}Th decays. As a result, the radioactivity of this parent nuclide decays slowly whereas the daughter is created at a faster rate (Masok *et al.*, 2018). These concerns could include a variety of ailments brought on by high-concentration ingestion and inhalation, including cancer, eye issues, epilepsy conditions, and others (Davies and Mundalamo, 2010).

2.1.1 Mining as the source of pollution

Uranium is used for nuclear energy production as a natural resource (Worlanyo and Jiangfeng, 2021). The demand for uranium mining has increased highly during World War II, and decreased in the last decade after World War II (Durand, 2012). Countries like South Africa have a need for the economic development that depends on mining, however there is a major

role in continuous challenges for uranium to be mined in the most responsible way (Winde *et al.*, 2017).

Mining in South Africa is a significant economic driver that provides economic opportunity for people (Hilson and Clifford, 2010). Mining is a significant anthropogenic activity that brings economic and social benefits such as employment, improved infrastructure as well as industrial developments (Worlanyo and Jiangfeng, 2021). However, its negative impact on society is expected to increase if the country does not follow proper safety procedures and enforce regulations (Winde *et al.*, 2017). Despite South African mines being the economic driver for the country, the mining processes have been producing numerous tailings which have high concentration levels of uranium (Worlanyo and Jiangfeng, 2021, Winde and Van der Walt, 2004). To date, commendable studies have found high concentrations of radionuclides and heavy metals in rivers due to discharge of efluent water from mines (Ajibade *et al.*, 2021, Manyatshe *et al.*, 2017, Van Rensburg *et al.*, 2016).

Compared to other countries, South Africa consists of several reserves which are considered the largest (Davies and Mundalamo, 2010, Worlanyo and Jiangfeng, 2021, Postar, 2017, Mudd, 2008). Processing of uranium started as a by-product of gold mining in the mining fields of the Witwatersrand area of Gauteng Province of South Africa. This was started by the Nuclear Fuels Corporation of South Africa (NUFCOR) in 1967 (Hanto *et al.*, 2022, Li *et al.*, 2022).

Extraction of uranium from the earth is not easy compared to diamonds or gold (Khumalo and Mathuthu, 2018). The element of uranium firstly needs to be transformed in preparation for sale (Mathuthu *et al.*, 2021). Milling is a chemical process used in mines to treat uranium. After the milling process, the chemical form is triuranium octoxide (Dutta *et al.*, 2022). The final process concentrates a mixture of uranium oxide in a form of a yellow cake (Dehdashti *et al.*, 2020). These milling processes produce nuclear waste from the mill tailings and waste containing heavy metals (Postar, 2017, Mudd, 2008). The heavy metals and radioactive chemicals contaminate the environment and water due to the radium decay to radon gas (Khan *et al.*, 2022). The decay series can potentially pose radioactive risk through blown dust particles, which result in inhalation effects on the environment and the nearby area (Mudd, 2008).

2.1.2 Potential impacts of uranium mining

The main uranium component in the nuclear fuel cycle plays a significant role in nuclear power plants by generating electricity and manufacturing nuclear weapons (Issah and Umejesi, 2018). Mining of uranium can potentially cause environmental pollution to the nearby water courses and areas through heavy metal and radionuclide chemical concentrations (Madzunya *et al.*, 2020). According to Mathuthu *et al.* (2021), uranium mining generates a large amount of waste rock and milling tailings (Díaz-Morales *et al.*, 2021). The risks associated with uranium mining include high concentration levels of background radiation, radioactive dust, and the release of radon gases which cause several impacts on the environment and humans (Bezuidenhout, 2021). Mining tailings needs to be disposed of and stored properly because leakage and emission of radiation from its waste can last for centuries in soil or water (Joyce, 2018). The mining tailings if, not disposed and stored properly, can result in contamination of the soil, surface and groundwater with uranium and heavy metals (Lindman *et al.*, 2020).

Excessive radionuclide concentration can lead to health effects such as lung cancer (Wolkersdorfer *et al.*, 2021). Exposure to uranium from breathing in fractured sand particles result in several effects such as lung cancer and kidney damage (Madzunya *et al.*, 2020). Radiation and heavy metals can, directly and indirectly, affect humans through inhalation of dust, contact with soil and water, as well as an intake of food such as fish and drinking of contaminated water (Ma *et al.*, 2020). To date, uranium mining activities tend to affect the surroundings socially and environmentally indirectly or directly through inhalation of dust, skin contact and ingestion of uranium concentrated particles (Mathuthu *et al.*, 2021, Madzunya *et al.*, 2020).

Naturally, isotopic ratios of uranium particles are in three parts of ^{238}U, ^{235}U and ^{234}U. The uranium element transforms to other elements in a slow process that can last for a period of hundreds to thousands of years (Ntsohi *et al.*, 2021). The transformation process of uranium to other elements is called the decay series (Mhlongo *et al.*, 2018). Uranium is not the only radioactive element, however, decay progeny of (Th) thorium, (Rn) radon, (Pb) lead, and (Po) polonium are also present in uranium ore as shown in figure 2.2. These decay products are considered toxic and radioactive (Masok *et al.*, 2018, Madzunya *et al.*, 2020).

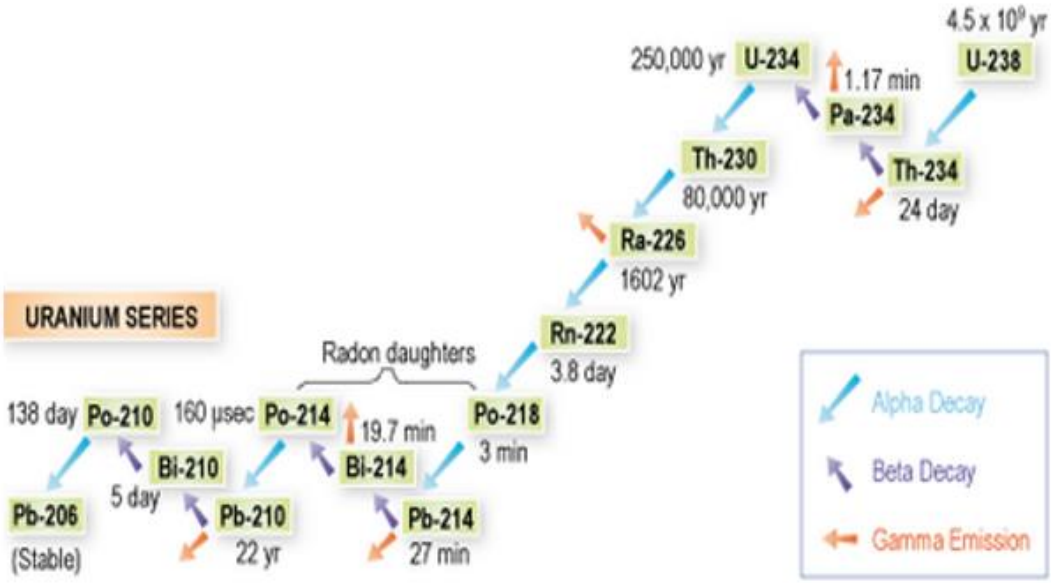

Figure 2. 3: Decay series of 238U (Ordóñez *et al.*, 2019)

The risks of radiation exposure do not depend entirely on the amounts of radiation exposed (Groffen *et al.*, 2018). The exposure can be small and cause minor damage that potentially contributes to cancer over a long period, or large and cause severe cancer in a shorter space of time (Madzunya *et al.*, 2020). As the earth disperses radiation naturally, humans are also exposed to the radiation in small amounts (Khumalo and Mathuthu, 2018). This radiation is called natural background radiation and cannot be avoided (Genthe *et al.*, 2018).

2.2 Potential pathways of pollutants

The potential pathway illustrates how pollutants, including radionuclides and heavy metals, move from their sources to the end receiver, such as people, by moving through the environment (Khan *et al.*, 2022). These putative paths include four characteristics such as environmental contamination, environmental medium, point of exposure and exposure pathway (Khan *et al.*, 2022). The gold mine tailings are regarded as a potential environmental pollution source (Mathuthu *et al.*, 2021). In some instances, fissure water from underground mine workings may occasionally be treated in water-purification facilities and utilized for human consumption (Khumalo and Mathuthu, 2018). If fissured water comes into contact with oxidized ore, it could become contaminated (Ojekunle *et al.*, 2022). Process water used in mining operations is another cause of contamination (Madzunya *et al.*, 2020). It typically includes dissolved toxins that may someday harm people if they were released into the

environment through evaporation, seepage, or run-off (Khan *et al.*, 2022). Other sources include settling ponds, evaporation dams, return-water dams, storm water drainage systems, and rock dumps (Van Rensburg *et al.*, 2019).

The environmental medium is the second pathway, where the contaminant passes through areas where human exposure is possible (Dutta *et al.*, 2022). If this occurs, the radionuclides and heavy metals may either dissolve or flow through run-off into surface water bodies or be leached into the underlying groundwater aquifers, poisoning water sources (Khan *et al.*, 2022). Water, air, food, and soil are the main environmental media for people. When taken as surface and/or groundwater, humans are exposed to radionuclides and heavy metals. Both surface water and groundwater can be used for drinking, bathing, farming, or recreational activities (Gani *et al.*, 2021, Liu *et al.*, 2022). The atmosphere can also expose people to contaminated indoor and outdoor air, such as wind-borne dust from mining waste (Liu *et al.*, 2022). Human exposure can also be increased by food that comes from polluted soil or water. Dusty soil that is blown into the air can also be deposited on food, which people may then eat or breathe in (Dutta *et al.*, 2022). The point of exposure is the third pathway (Liu *et al.*, 2021). Here, a contaminant comes into contact with the body. At this point, people might be exposed to radionuclides and heavy metals, for instance, in their workplaces, rivers, or residences. This can happen either through ingestion or breathing (Gani *et al.*, 2021, Liu *et al.*, 2022).

The exposure pathway is the fourth one. It explains how a contaminant enters the body of a human. In general, there are different ways that radionuclides and heavy metals might enter a person's body (Marara and Palamuleni, 2019). These include ingesting or swallowing food or water that has been contaminated or inhaling a gaseous substance, like radon gas. It is possible to inhale small amounts of dust into the lungs. The dermal skin contact is another pathway, wherein the contaminated material is absorbed through the skin from the water, soil, or air (Khan *et al.*, 2022).

2.3 Heavy metals

Heavy metals are considered the environmental sources of pollution (Ugochukwu *et al.*, 2022). Activities caused by humans such as mining and waste water discharges leave high concentrations of heavy metals in soil and water (Zhou *et al.*, 2020b). The heavy metals in soil can pass into the aquatic environment, groundwater and plants, reaching humans and animals (Zhou *et al.*, 2020b). Heavy metals are found everywhere due to natural and anthropogenic

activities (Bird *et al.*, 2005). They have a specific gravity that is greater than 5 g/cm classification. Such classifications include metalloids, lanthanides, basic and transition metals, actinides and metals of groups III to V of the periodic table. (Edokpayi *et al.*, 2022). The examples of these classifications include arsenic (As), cadmium (Cd), aluminum (Al), copper (Cu), chromium (Cr), cobalt (Co), iron (Fe), mercury (Hg), lead (Pb), manganese (Mn), selenium (Se), zinc (Zn) and Nickel (Ni) (Edokpayi *et al.*, 2022).

Heavy metals are easily transferred from one place to another and are very persistent in the environment (Khan *et al.*, 2022, Rani *et al.*, 2022). As a result, they get to be ingested by humans through food and water (Edokpayi *et al.*, 2022). Their toxic level depends on the dose absorbed and the type of metal (Klubi *et al.*, 2020). Some heavy metals, even in small amounts, can cause illness in the human body and affect body organs (Klubi *et al.*, 2020). Their effects on humans include diseases such as tuberculosis, asthma and gastrointestinal diseases (Durand, 2012, Jibiri and Okeyode, 2012, Moloi *et al.*, 2020).

2.3.1 Heavy metals in rivers

Rivers across the world play an important part in supplying humanity with the domestic water they require (Khan *et al.*, 2022). However rivers may contain high levels of heavy metals, which are poisonous and non-biodegradable and pose substantial dangers even at low quantities (Rani *et al.*, 2022). The extraction and processing of metal ores have been linked in numerous studies to the pollution of river ecosystems with heavy metals (Bird *et al.*, 2005, Dehdashti *et al.*, 2020, Díaz-Morales *et al.*, 2021, Edokpayi *et al.*, 2022). Metals can also be released naturally into the environment, but other events such as mining, direct waste dumping into the river, erosion and pollution into the river potentially cause higher metal concentrations (Bird *et al.*, 2005, Díaz-Morales *et al.*, 2021).

Rivers can also contain metalloids such as selenium, which can be toxic at low exposure levels (Edokpayi *et al.*, 2022). Mining and smelting operations, industrial production and consumption, residential and agricultural usage of metals and metal-containing compounds all result in metal exposure, which has a negative influence on the environment. (Wolkersdorfer *et al.*, 2021). Some of the environmental hazards related to these heavy metals include metal ion deposition in the air and soil, as well as heavy metal leaching and sediment re-suspension (Ashraf *et al.*, 2020, Choudhury *et al.*, 2022, Ugochukwu *et al.*, 2022). In addition, one of the natural processes that contributes to the pollution of heavy metals is weathering (Mhlongo *et*

al., 2018) wherein rocks and minerals breakdown or dissolve into the environment over a period of time (Zhou *et al.*, 2020b).

2.3.2 The effects of heavy metals

Some metals, like iron and copper, are essential to human life because of their indispensable functions in the operation of body organs (Khaleeq *et al.*, 2022). It is crucial to remember that all living things require different levels of heavy metals, which turn poisonous when ingested in high doses (Rani *et al.*, 2022). Lead (Pb) is one example of a metal that may be toxic even at low exposure levels (Morales-Silva *et al.*, 2022). It is also listed as harmful on the United States Agency for Toxic Substances and Disease Registry's priority list of heavy metal pollutants (Johnson, 1995, Przybyla *et al.*, 2021).

The environment, water, and soil may get contaminated by heavy metals from mining operations (Tomno *et al.*, 2020). Increased heavy metal uptake by crops may result from an excessive buildup of heavy metals in the soil (Ugbede *et al.*, 2021). Food and drink can also include heavy metals (Ojekunle *et al.*, 2022), which can then be transported throughout the body's tissues and organs after being absorbed (Dutta *et al.*, 2022). Once absorbed, they are dispersed throughout tissues and organs and may deposit in the bones, kidneys, liver, and lungs, posing major health dangers (Singh *et al.*, 2022, Tomno *et al.*, 2020).

Lead (Pb) is harmful even in low quantities because it builds up over time and is thought to be mutagenic and perhaps carcinogenic to humans (Khan *et al.*, 2022, Dan *et al.*, 2022). Pb frequently enters river water through lead pipes, faucets, and plumbing equipment (Manyatshe *et al.*, 2017). According to the world average permissible limit, Pb in soil and water should not exceed 0.05 and 85 ppm respectively (WHO, 2022). Pb has hazards, including but not restricted to kidney tumours, delayed cognitive maturation, and raised blood pressure in adults (Choudhury *et al.*, 2022). Additionally, Pb toxicity has the ability to reduce the production of haemoglobin, which would interfere with the normal operation of the kidney, joints, reproductive, and cardiovascular systems and result in long-term harm to the central and peripheral nerve systems (Sylvie Désirée *et al.*, 2021). The neurotoxic effects of Pb appear to be most dangerous to growing foetuses and children (Morales-Silva *et al.*, 2022). According to (Devi and Mehendale, 2014) children under the age of five who are exposed to low levels of Pb may experience delays in their intellectual development.

Phosphorus (P) is crucial for the development of bones and teeth and is used extensively by the human body to process carbohydrates and lipids (Runcie and Larkum, 2001). Additionally, the body needs protein for the development, upkeep, and healing of cells and tissues (Buzetzky *et al.*, 2023). However, phosphorus intake that is too high can be harmful to the general health of people, plants, and animals (Skerratt-Love *et al.*, 2023). A phosphorus imbalance in humans may lead to osteoporosis (Tarasova *et al.*, 2022). According to the world average permissible limit of P in soil and water, the recommended limit of 50 ppm in soil and 0,05 ppm in water (WHO, 2022) should not be exceeded. Algae can grow more quickly than ecosystems can tolerate when there is too much phosphorus in the water. Significant increases in algae have an impact on habitats, food supplies, and water quality (Runcie and Larkum, 2001). They also reduce the amount of oxygen that aquatic life requires to exist. Algal blooms are huge growths of algae that can drastically diminish or completely remove oxygen in the water, causing diseases in fish and the demise of large numbers of fish (Tarasova *et al.*, 2022). Some algal blooms are dangerous to people because they increase the production of toxins and germs that can make people sick if they come into contact with contaminated water, eat ruined fish or shellfish, or drink contaminated water (Zhao *et al.*, 2022).

Haemoglobin, a protein that transports oxygen in the blood, depends on iron (Fe) (ThomasArrigo and Kretzschmar, 2022). In addition, iron is important in a number of other critical bodily functions (Lin and Liu, 2022). A lack of iron in the blood can result in a number of serious health issues, such as iron deficiency anaemia (da Silva *et al.*, 2022). Despite being a component of drinking water, iron is rarely found at amounts higher than 10 mg/L, or 10 ppm (Liu *et al.*, 2021, Lin and Liu, 2022). The permissible limit in soil is 50 ppm while in water, the suggested limit is 0.3 mg/l (ppm) (WHO, 2022). The presence of iron in water is determined more by taste and appearance than any negative effects on health (Van Rensburg *et al.*, 2019). However, water can turn reddish-brown with as little as 0.3 mg/l of the substance present. When iron is mixed with tea, coffee, and other liquids, it results in an unfavourable flavour and an inky, black look (ThomasArrigo and Kretzschmar, 2022). When vegetables are cooked in water with too much iron, they turn black and appear unpleasant. Even though low iron levels are not harmful to your health, water contain micro-organisms that could be harmful to the human body (Zhang *et al.*, 2022). Additionally, a high iron level in the water results in an overload that might result in diabetes, hemochromatosis, stomach issues, and nausea. It can also harm the heart, liver, and pancreas (Zhang *et al.*, 2022).

Manganese (Mn) is a trace mineral that is predominantly found in bones, the liver, kidneys, and pancreas of the human body (da Silva *et al.*, 2022). Manganese aids in the formation of bones, connective tissue, blood clotting factors, and sex hormones in the body (Plessl *et al.*, 2019). The suggested limit in water is 0.05 ppm and soil, 5 ppm (WHO, 2022). Long-term consumption of manganese-rich water can impair memory, attention, and motor skills in children and adults. If infants drink too much manganese-containing water, they could potentially experience behavioural and developmental issues (Moloi *et al.*, 2020). Manganese toxicity has the potential to cause a neurological condition with long-term symptoms like tremors, trouble walking, and facial muscle spasms (Plessl *et al.*, 2019). These symptoms are frequently followed by other, more minor ones, such as agitation, aggression, and hallucinations (Moloi *et al.*, 2020).

Another element, selenium (Se) is primarily found in soil. It has been used to treat thyroid autoimmune disease and excessive cholesterol (Plessl *et al.*, 2019). It is present as water-soluble selenite in alkaline soils and is easily accessible to plants. Not only that, but it is typically found as selenite linked to iron and aluminium oxides in acidic soils, where its solubility is typically quite low (Plessl *et al.*, 2019). Its limit in soil is 0.4 ppm, while in water is 0.01 ppm (WHO, 2022). However, this mineral aids in protecting the body from oxidative stress damage and is essential for thyroid and metabolism function. Selenium may strengthen the immune system, minimize the effects of ageing on cognitive function, and even lessen heart disease issues (Genthe *et al.*, 2018, Dehdashti *et al.*, 2020). Exposure to it can cause symptoms like nausea, vomiting, nail discolouration, brittleness, hair loss, exhaustion, irritability, and bad breath (Plessl *et al.*, 2019).

Despite being a necessary micronutrient for plant growth, boron (B) has the potential to be harmful in high concentrations (Vera *et al.*, 2021, Vera *et al.*, 2019, Ramos *et al.*, 2021). The suggested concentrations in water are set at 2 ppm and soil, 4 ppm (WHO, 2022). When inhaled as dust, boron compounds can be somewhat hazardous, causing inflammation and itchiness but little long-term harm (Vera *et al.*, 2019). Anorexia, hypothermia, restlessness, fatigue, renal damage, dermatitis, alopecia, and indigestion are other symptoms of borate poisoning (Vera *et al.*, 2021). High doses of boron exposure can disrupt the male reproductive system, lower foetal weight, and cause abnormal foetal development (Das *et al.*, 2019).

Cobalt (Co) is a known necessary micronutrient for maintaining the neurological system and producing red blood cells (erythropoiesis) (Suh *et al.*, 2019). Depending on the amount and

duration, cobalt exposure at high levels may be harmful to people (Córdova-Lizama *et al.*, 2022). The suggested and safe amount of exposure to Co is 1.5 ppm in water, while in soil it is 50 ppm (WHO, 2022). An asthma attack with shortness of breath, wheezing, coughing, and chest tightness can also be brought on by prolonged exposure. In addition, it may cause failure of the thyroid, liver, kidney, heart, and other organs (Moloi *et al.*, 2020, Córdova-Lizama *et al.*, 2022). Chronic inhalation of cobalt dust can harm the eyes, skin, heart, and lungs as well as produce fibrosis, which is a type of lung scarring (Bamana *et al.*, 2021).

Lithium (Li) is a medication that helps stabilize mood and is used to treat mood disorders such as mania (which is characterized by feelings of extreme excitement, hyperactivity, or distraction) and hypomania (which is a milder form of mania) (Yousefi *et al.*, 2014, Robinson *et al.*, 2018, Chaves *et al.*, 2021). Bipolar depression can also be treated with it. Thyroid function may be impacted by lithium consumption from food, water, or other environmental sources (Aral and Vecchio-Sadus, 2011). The safe exposure of Li in soil is 30 ppm, while in water it is 5 ppm (WHO, 2022). The signs of Li poisoning include severe hand tremors, confusion, vision abnormalities, and severe nausea and vomiting (Bolan *et al.*, 2021, Avila-Arias *et al.*, 2019).

One metal at its suggested concentrations in water that is 0.1 ppm and soil 30 ppm (WHO, 2022), nickel (Ni), has been linked to cancer, as well as oral and intestinal issues (Avila-Arias *et al.*, 2019). Depression, heart attacks, hemorrhages, and kidney issues could all result from it (Mokarram *et al.*, 2020). In addition to the other elements, copper (Cu) at the recommended limit in soil of 36 ppm and water 0.01 ppm and zinc (Zn) in soil at 50 ppm as well as water at 5 ppm are important elements that are necessary for life (WHO, 2022). The elements are crucial for the body's healthy operation. However, prolonged exposure could possibly have negative effects on people who are not cancerous (Mokarram *et al.*, 2020). Cu keeps the human immune system and nerve cells healthy and aids in the production of red blood cells. A surplus of Cu has been linked to liver damage, while Zn and Cu interact negatively. Inhibition of development and reproduction may also occur at higher Zn concentrations (Rani *et al.*, 2022).

2.4 Instruments that are commonly used for heavy metal analysis

Different analytical methods, including Neutron Activation Analysis (NAA), Proton Induced X-Ray Emission Spectroscopy (PIXE), X-Ray Fluorescence Spectroscopy (XRF), Atomic

Absorption Spectrometry (AAS), Ion Chromatography (IC) and Inductively Coupled Plasma-Mass Spectrometry (ICP-MS) can be used to analyse heavy metals (Madzunya *et al.*, 2020).

2.4.1 Neutron Activation Analysis (NAA)

NAA is a non-destructive method for performing major quantitative analysis and tracing elements in samples that involves irradiating sample material with neutrons in a nuclear reactor (Sayam *et al.*, 2023). NAA provides for discrete sampling of elements because it disregards the chemical form of a sample and concentrates purely on atomic nuclei. The approach is based on neutron activation and consequently requires a neutron source (Truong *et al.*, 2022, Salgado *et al.*, 2023). The sample is bombarded with neutrons, which causes its constituent elements to produce radioactive isotopes (Sayam *et al.*, 2023, Cui and Yang, 2023). Using this information, it is possible to examine the spectra of the radioactive sample's emissions and determine the amounts of the various elements contained inside it (Little *et al.*, 2020, Cui and Yang, 2023). This approach has the additional benefit of not destroying the sample. NAA can also be used to determine the concentration of a radioactive sample (Little *et al.*, 2020). Figure 2.3 shows the process of NAA applications.

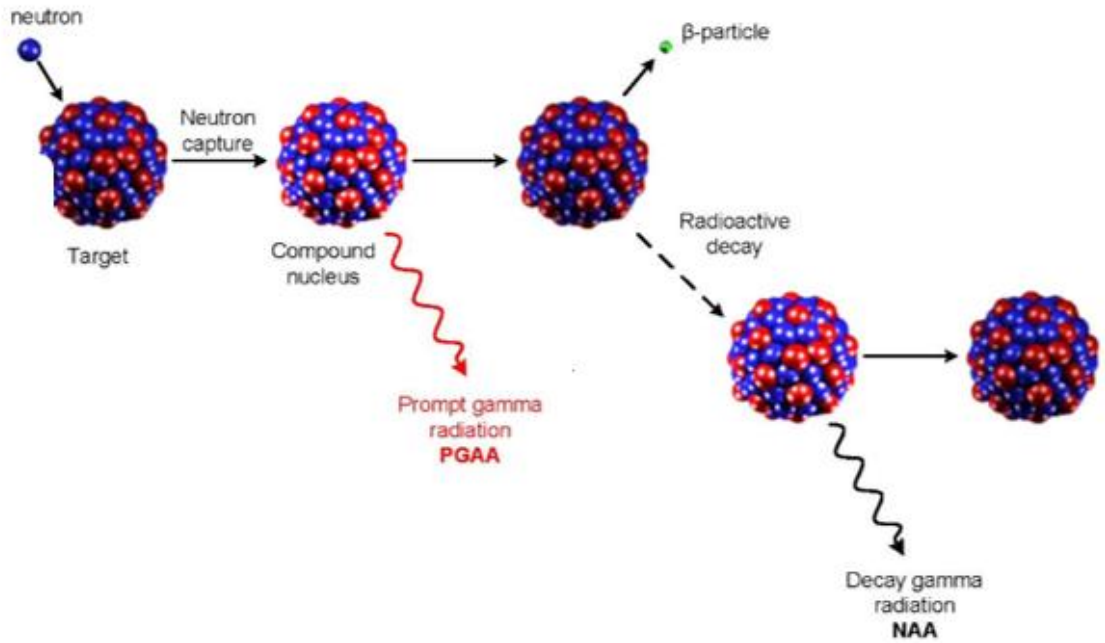

Figure 2. 4: Neutron Activation Analysis (Landsberger, 2022).

Despite the fact that the technique is essentially non-destructive, the irradiation sample will stay radioactive for many years after the initial analysis, requiring low- to medium-level

radioactive material handling and disposal protocols (Sayam *et al.*, 2023, Nangeelil *et al.*, 2023, Cui *et al.*, 2023). The need for a neutron source, as well as the extremely high cost of the analysis, are the main barriers to broad adoption of this approach (Cui and Yang, 2023).

2.4.2 Proton Induced X-Ray Emission (PIXE)

PIXE is a non-destructive analytic technique used to detect the elemental content of a sample using X-ray emissions induced by proton irradiation (Arai *et al.*, 2023). The process includes irradiating a substance with protons accelerated to energies ranging from 2 to 5 MeV (Satyanarayana *et al.*, 2022, Zhang *et al.*, 2021). Accelerated protons collide with inner orbital electrons (K or L orbital) of the elements in the sample under analysis, resulting in a cascade of electrons falling from outer higher-energy orbitals to inner orbitals and the simultaneous emission of X-radiation at energy lines specific to each element (Hatam *et al.*, 2023, Arai *et al.*, 2023). A suitable X-ray detector, such as a silicon drift detector, is used to measure the intensities of the X-rays generated by the sample, allowing the elements in the substance under study to be identified and measured (Zhang *et al.*, 2021). The elements are recognized using the characteristic X-ray energy lines of each element, and the X-ray intensities at certain energies are utilized to quantify each element in the sample under analysis (Satyanarayana *et al.*, 2022). Pure element standards are used to calibrate the X-ray detector response to X-rays generated by the sample at different energy lines (Satyanarayana *et al.*, 2022, Zhang *et al.*, 2021). The figure 2.4 shows PIXE processes in reaction to the proton.

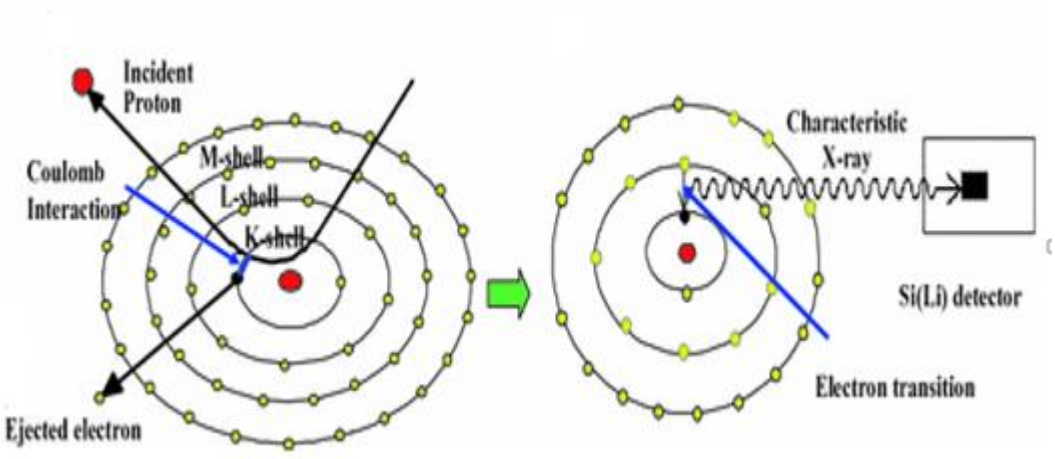

Figure 2. 5: PIXE (Sera, 2018).

Elements lighter than magnesium (atomic number 12) are unlikely to appear in a PIXE spectrum. As a result, PIXE is more suited to detecting the composition of heavy metals rather than organic components (Sera, 2018, Arai *et al.*, 2023).

2.4.3 Atomic Absorption Spectrometry (AAS)

AAS is an analytical technique used to determine the concentration of particular elements in a sample (Vista, 2015). AAS detects elements in liquid or solid samples by using certain wavelengths of electromagnetic radiation from a light source. Individual elements absorb wavelengths differently, and the absorbency of these elements are evaluated against standards. This is based on the principle that atoms (and ions) may absorb light at a single, unique wavelength. When this exact wavelength of light is delivered, the energy (light) is absorbed by the atom. A simple presentation of this is shown in figure 2.5

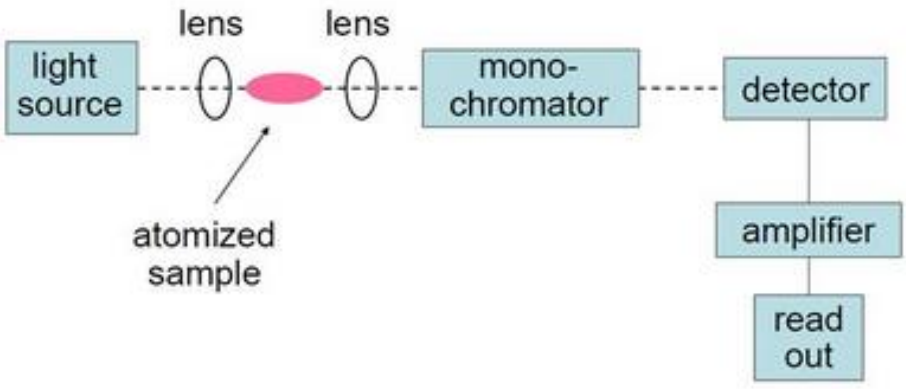

Figure 2. 6: Schematic diagram of AAS (Masac *et al.*, 2021).

The technique is easy to operate with high sensitivity as it can detect up to parts per billion (ppb), however it is quite expensive and samples are destroyed in the process. One of the main drawbacks of this technique is its ability to only measure one element at a time.

2.4.4 Ion Chromatography (IC)

Ion chromatography is a liquid technique wherein atomic and molecular ions are separated for examination using ion exchange compounds (Huang *et al.*, 2023). The technique is used in

environmental samples to separate and analyse anions and cations in lower concentrations of parts per billion (ppb) (Zhu *et al.*, 2023, Li *et al.*, 2023). It can detect concentrations of anions such as fluoride, chloride, nitrate, nitrite, and sulfate, as well as cations such as lithium, sodium, ammonium, potassium, calcium, and magnesium (Schorr *et al.*, 2023).

The ion detector generates a chromatogram that shows the relationship between conductivity and time, as shown in figure 2.6. Each ion causes a peak to appear, wherein the height is determined by the relative ion concentration in the injected solution (Worden, 2005).

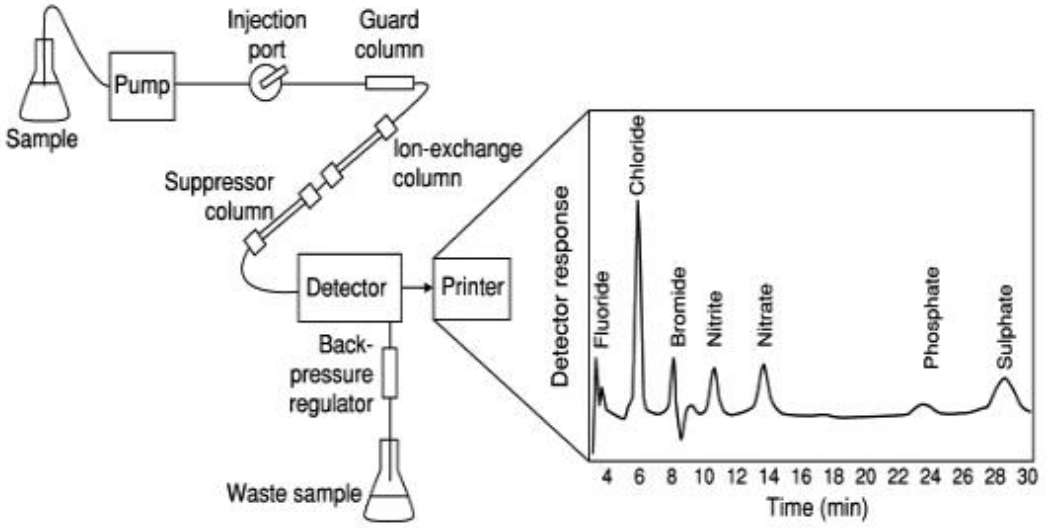

Figure 2. 7: Schematic diagram of IC (Worden, 2005).

Ion chromatography is currently one of the quickest and most accurate techniques that analyses different samples (Li and Liu, 2019). Chromatography enables precise separation, analysis, and purification. It can identify pharmaceuticals, food particles, plastics, pesticides as well as air and water samples, among other things, with a very small sample (Abusultan *et al.*, 2023, Paull and Michalski, 2019). Despite its benefits, Ion Chromatography has certain drawbacks. One of the major disadvantages is the lack of universal detection (Yates *et al.*, 2023). The technique cannot provide structural information about the separated species, however it is often preferred due to its sensitivity to ions (Paull and Michalski, 2019).

2.4.5 Inductively Coupled Plasma-Mass Spectrometry (ICP-MS)

ICP-MS was employed in this investigation to analyse the presence of heavy metals in environmental samples. The low detection limit, lower interference, and quick multi-element

analysis are the key benefits of utilizing this technique. Figure 2.7 shows the image of the ICP -MS technique used in this study.

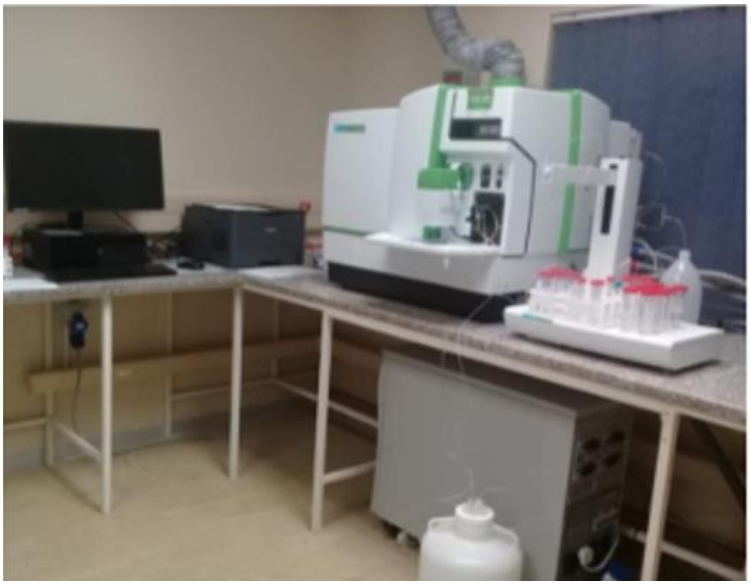

Figure 2. 8: The Perkin Elmer, NexION 2000 ICP-MS at CARST

The ICP system and the MS system make up ICP-MS. The atomization of the sample in question is one advantage of the ICP system (Madzunya *et al.*, 2020). The liquid sample is atomized into plasma using a nebulizer. To do this, argon that rotates when exposed to the liquid sample is mixed with the liquid sample. The mass spectrometry (MS) system is mostly used for atom separation. The various parts of the ICP-MS system are depicted in Figure 2.8.

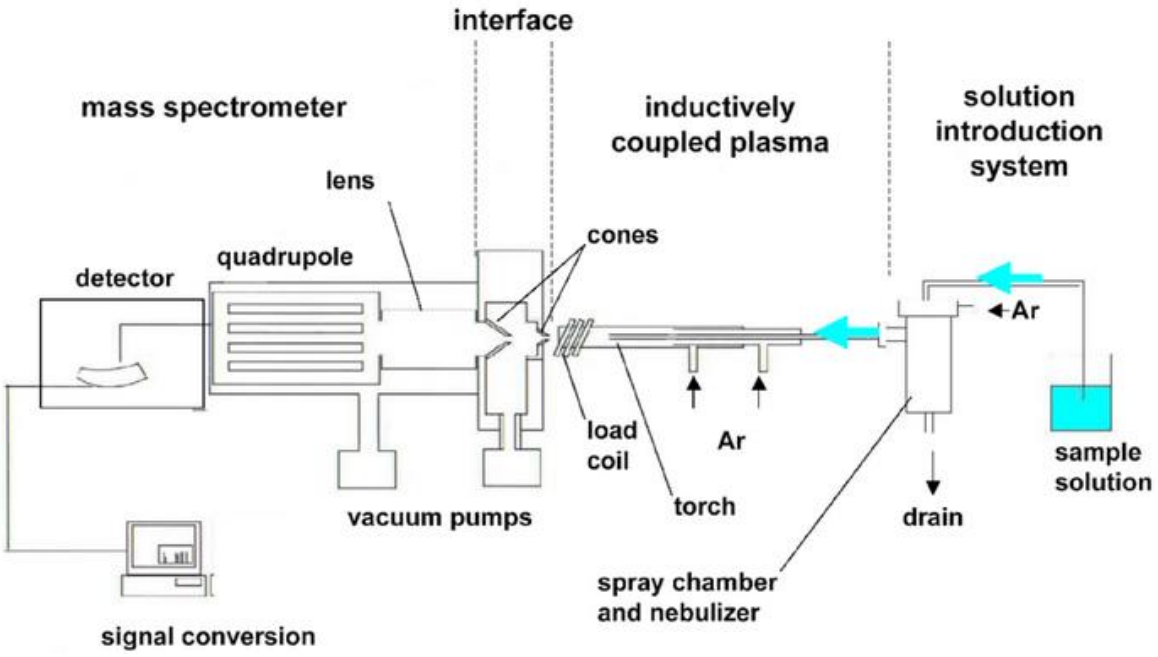

Figure 2. 9: Sample schematic of an ICP-MS instrument (Williams and Pillay, 2011).

The mechanism for introducing samples is the first part of the ICP-MS as shown in figure 2.8. This is made up of a nebulizer and a spray chamber, which offer a way to introduce liquid samples into argon plasma as tiny aerosol droplets. The liquid sample is broken up into tiny droplets by the high-velocity argon gas stream, which is then pumped into the spray chamber. The next element that produces the argon plasma is the ICP torch and coil. Atoms, ions, and electrons are placed in a highly hot environment (between 6000 and 10,000 Kelvin) by the plasma. Since there is enough energy to entirely eliminate an element's outer shell electrons, many elements go from the atomic to the ionic form at these temperatures. As a result, the plasma separates the molecules from the aerosol, dries the aerosol, and then takes the electrons out of each component to create singly-charged ions, which are then sent into the mass spectrometer for mass filtration (PerkinElmer, 2004-2011). Figure 2.8 shows the schematic image of ICP-MS.

The interface then connects the high vacuum mass spectrometer to the atmospheric pressure ICP ion source. The interface is where the plasma's ions are removed and supplied to the mass spectrometer as an ion beam. High vacuum is used to operate the quadrupole, the detector, and the ion optics. The sampled ions are accelerated and concentrated onto the mass filter by a group of charged plates or ion lenses once they have reached the high vacuum area of the mass spectrometer. Ion optics make sure that neutral species and photons are removed from the ion beam while guiding the targeted ions towards the mass analyser (quadrupole) (PerkinElmer,

2004-2011). Before the ion beam enters the mass spectrometer, it passes through the collision or reaction cell, which is used to filter out interferences that could reduce the range of detection that is possible.

Ions are sorted according to their mass-to-charge ratios using the mass spectrometer as a mass filter. A quadrupole mass spectrometer is used in the majority of commercial ICP-MS systems to quickly check the mass range. One mass-to-charge ratio at a time is permitted to move from the entry to the exit of the mass spectrometer. Ions are bent as they enter the MS system by the perpendicular magnetic and electric fields that are associated to it. The mass of the ions affects how wide the arch is. As they travel to the detector, the ions are divided based on their mass-to-charge ratios. Ions leave the mass spectrometer and hit the first denode of a detector called an electron multiplier. Individual ions leaving the quadrupole are counted by the detector.

A stream of electrons is created when the ions collide; these electrons are then amplified until they generate a detectable pulse. The data handling and system controller is the final element that manages all facets of instrument control and data handling. In order to calculate the element's concentration, a calibration curve must be created by comparing the measured pulse intensities to standards using Perkin Elmer's Syngistix Version 5.0 software. The concentrations of analytes in the aqueous sample are proportional to the detected ion intensities at various masses (Madzunya *et al.*, 2020).

2.5 Radionuclides

Radionuclides are recognized to exist naturally or to be manufactured artificially in nuclear reactors, cyclotrons, particle accelerators, or radionuclide generators (Yan *et al.*, 2021). Although radiation naturally occurs at a level that is not dangerous to human health (Petrosyan and Perikhanyan, 2022), there is a significant worry for the environment, the ecosystem, and people due to radionuclides that are increased by anthropogenic activities like mining (Moshupya, 2022). Recently, high concentrations of radionuclides have attracted interest as a topic of discussion (Moshupya, 2022, Zupunski *et al.*, 2023). Products derived from radionuclides such as uranium are utilized extensively in a variety of fields, and people who are not occupationally exposed are potentially affected even at relatively small doses in their daily lives (Winde *et al.*, 2017).

There are categories of radionuclides that depend on their point of origin, like cosmogenic radionuclides produced by the interaction of cosmic rays with the earth's atmosphere (Bloch

and Owusu, 2012). Radionuclides like ^{14}C, ^{7}Be, ^{22}Na and ^{3}H are created as a result of these cosmic ray's interactions with stable nuclides in the atmosphere (Jibiri and Okeyode, 2012). The second group consists of terrestrial radionuclides, which are thought to be primordial because of their lengthy half-lives of about four billion years (Bloch and Owusu, 2012). These radionuclides comprise ^{235}U, ^{238}U, ^{232}Th and ^{40}K among others. The decay chain of ^{235}U, ^{238}U and ^{232}Th are known as daughter progenies (Aichinger *et al.*, 2012). They are known to persist in the tissues of all living things, as well as in the crust of the earth (Kathren, 1998). The final group is referred to as "anthropogenic" radionuclides, which are produced as a result of human endeavours including mining and commercial manufacturing of radiopharmaceuticals (Bloch and Owusu, 2012).

Due to their lengthy half-lives of (>100 million years), which have not yet fully decayed, primordial radionuclides like uranium (U) and thorium (Th) still exist today (Ordóñez *et al.*, 2019, Rutgers van der Loeff, 2019). For the majority of practical purposes, radionuclides with half-lives that are numerous times longer than the age of the universe can be regarded as stable (Ashok *et al.*, 2019). Most significantly, the discovery of this degradation in bismuth-209 meant that bismuth was no longer thought to be stable (Franchi *et al.*, 2022). The list of primordial radionuclides could grow as decay is seen in daughter nuclides (Novikau and Lujaniene, 2022, Yan *et al.*, 2021). Bismuth 209 occurs in the Neptunium decay chain, as shown in figure 2.9.

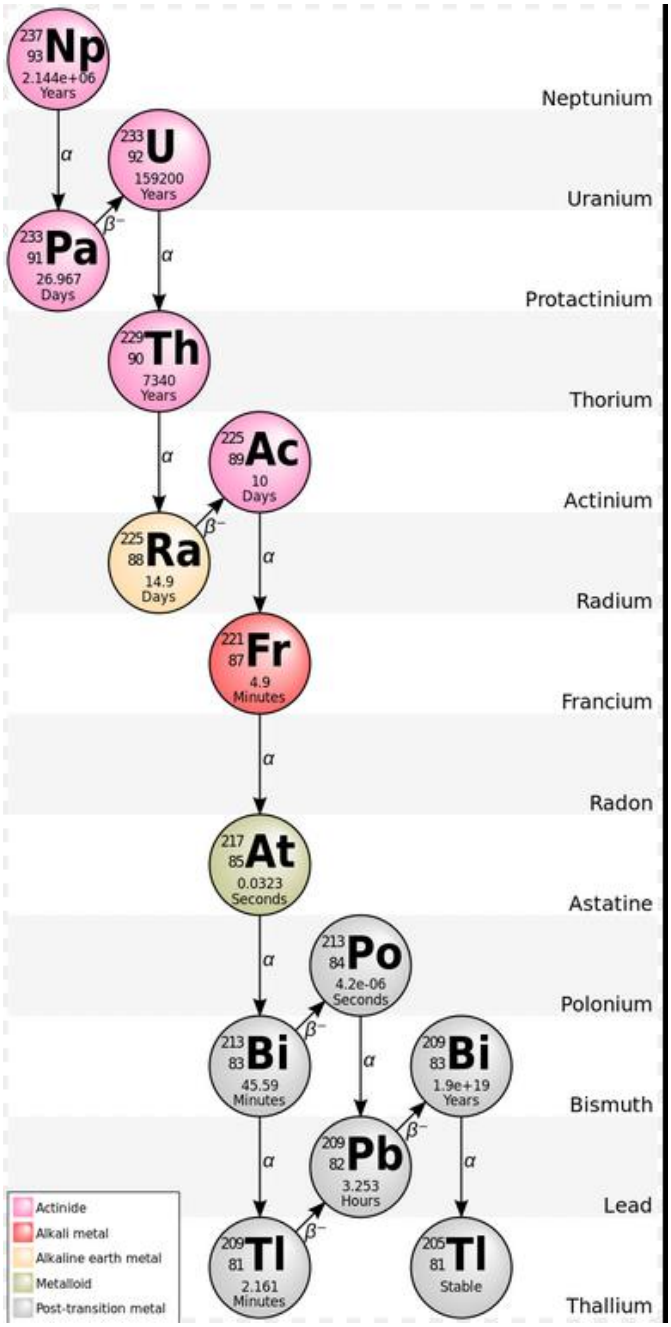

Figure 2. 10: Bismuth 209 neptunium chain (Franchi *et al.*, 2022)

The decay of primordial radionuclides produces radiogenic isotopes known as terrestrial radionuclides (Kamunda, 2017). Compared to primordial radionuclides, they have shorter half-lives. They emerge from the decay chains of the primordial isotopes ^{232}Th (thorium), ^{238}U (Uranium) and ^{235}U (Uranium) (Masok *et al.*, 2018). Examples include the naturally occurring isotopes of radon and polonium (Khumalo and Mathuthu, 2018). All of these cosmogenic nuclides are among the radionuclides that are only found in trace concentrations in nature

(Khumalo and Mathuthu, 2018). Short-lived radionuclides will be in short supply because secondary radionuclides will occur in proportion to their half-lives. Additionally, radionuclides can appear in nature in virtually undetectable amounts as a result of uncommon occurrences like spontaneous fission or peculiar interactions with cosmic rays (Yan *et al.*, 2021, Ravisankar *et al.*, 2015).

Although modest levels of exposure occur naturally without harming living things, including humans, unplanned exposure to radionuclides is often detrimental (Bloch and Owusu, 2012). The type and amount of radiation emitted, the amount and type of exposure (close contact, inhalation, or ingestion), and the element's biochemical characteristics will all have an impact on how much harm is caused (Khumalo and Mathuthu, 2018). However, nuclear medicine uses radionuclides with the right characteristics for both diagnosis and treatment. The several types of radionuclides, such as cosmogenic and primordial secondary radionuclides, indicate how they interact naturally on Earth (Yan *et al.*, 2021; Ravisankar *et al.*, 2014).

Additionally, radionuclides that enter the environment could have negative consequences, including radioactive pollution (Ravisankar *et al.*, 2015, Mathuthu *et al.*, 2021). Besides, they can harm living organisms if they are exposed to radiation poisoning or utilized excessively during treatment (Ravisankar *et al.*, 2015). Radionuclide exposure may cause health problems and impair the functions of healthy tissue or organs, depending on a number of circumstances (Madzunya *et al.*, 2020). Radiation exposure can result in a variety of effects, including acute radiation syndrome, radiation burns, and hair loss. Long-term exposure can cause cell damage, which can result in cancer (Zakaly *et al.*, 2021).

2.5.1 Key Radionuclides

Most of the information on important radionuclides is found in the U and Th series, especially for those with longer half-lives (Pourcelot *et al.*, 2021, Postar, 2017). In the majority of environmental samples, potassium (K) is simply identified and reported. It is a 1460 keV gamma emitter and is not significant radiologically (Madzunya *et al.*, 2020). A significant quantity of K is required for good plant growth, but too much K can be harmful since it may alter how the soil absorbs vital minerals. By reducing the K content of the soil, surplus phosphorus can be kept out of rivers, where it can promote the growth of algae that eventually threaten aquatic life. K is necessary for humans to have healthy nerves and muscles, especially

heart muscle cells (Singh *et al.*, 2020). Because low levels of K can be fatal, immediate medical care is necessary (Singh *et al.*, 2020).

Contrarily, there is no recognized biological use for thorium (Th) (Rutgers van der Loeff, 2019). The radioactivity of it is what makes it toxic. The risk of lung and pancreatic cancer is increased by breathing in Th dust, according to numerous research studies. Bone cancer risk is elevated in those who are exposed to Th (Masok *et al.*, 2018). Low concentrations of the radioactive metal thorium, which is present naturally, can be found in water, plants, animals, soil, rocks, and other living organisms (Yan *et al.*, 2021, Rutgers van der Loeff, 2019). ^{232}Th, ^{230}Th and ^{228}Th are the radioactive isotopes of thorium, which make up nearly all of its naturally occurring forms (Mathuthu *et al.*, 2021).

2 .6 Radiation detection instrument

When a nuclear particle enters a device to cause either excitation or ionization, the detection process begins. Radiation detectors come in a variety of shapes and sizes (Meert *et al.*, 2022). If a nuclear particle interacts with a specific substance and causes excitation followed by fluorescence de-excitation, light is released that can be detected by a scintillation detector (Cui and Yang, 2023, Barrientos *et al.*, 2011). Scintillation detectors have high acquisition efficiency but low resolution. It is possible to create solid, liquid, or gas scintillation detectors depending on the medium from which scintillation occurs (Sharma and Burnett, 2021).

The second kind of detector works by ionizing the space between its charged electrodes, which is how it generates charge carriers. The ion chamber, proportional, and Geiger-Müller tubes are the most common types of devices based on this principle (Harkness-Brennan *et al.*, 2014). They can also be made of solid semiconductor materials. P-n junction diodes are the structural type of solid semiconductor detectors. Applying a reverse bias voltage across a p-n diode causes a depletion area to form (Gruber *et al.*, 2009). Charge carriers (positive holes and negative electrons) are released as a result of photon interactions in the depletion zone and are then swept by a voltage supply to the appropriate collecting electrodes (Cui and Yang, 2023, Barrientos *et al.*, 2011). To create a voltage pulse with an amplitude corresponding to the initial photon energy, the collected charge is supplied into a preamplifier (Barrientos *et al.*, 2011).

The most widely used materials for semiconductor detectors are silicon (Si) and germanium (Ge) (Cui and Yang, 2023, Barrientos *et al.*, 2011). Because of several benefits, including high energy resolution, strong stability, great timing characteristics, and simplicity of operation,

semiconductor detectors are most frequently employed for gamma spectrometry (Sharma and Burnett, 2021). Between Ge and Si detectors, there are three key distinctions: the energy gap, the atomic number, and the mobility of the main carriers (Sharma and Burnett, 2021). In Ge, as opposed to Si, an electron-hole pair can be produced with less energy. Since some Si detectors can be used at ambient temperature, Ge detectors must be cooled to 77 K or -196 ^{0}C to get an acceptable level of leakage current caused by the thermal production of charged carriers (Tarasova *et al.*, 2022). In order to operate a Ge detector, it must be vacuum-operated and cooled to liquid nitrogen temperatures (Cui and Yang, 2023, Barrientos *et al.*, 2011). Thus, moisture and other pollutants that can condense are kept away from the sensitive detector surfaces (Sharma and Burnett, 2021).

A gamma detector is made with a high photoelectric cross-section material for increased efficiency (Barrientos *et al.*, 2011). Because the photoelectric cross-section is proportional to the fifth power of the atomic number Z, Ge outperforms Si by one to two orders of magnitude (Harkness-Brennan *et al.*, 2014). Gamma-spectroscopy is a critical, non-destructive method for measuring gamma radiation from various radionuclides in environmental samples (Choudhury *et al.*, 2022). Many radioactive sources emit rays of varying energies and probabilities of emission (Hung *et al.*, 2017). These gamma lines are gathered into a spectrum and analysed using a gamma spectrometry system (Cui and Yang, 2023, Barrientos *et al.*, 2011). In this study, the soil samples were that were analysed using the Broad Energy Germanium Gamma Spectrometer, are not reported.

2.6.1 Broad Energy Germanium (BEGe) Gamma Spectrometry

The interaction properties of gamma rays with the absorbing material are used to detect gamma photons in this instrument (Barrientos *et al.*, 2011). The photoelectric effect, Compton scattering, and pair production are the three major processes by which gamma rays interact with the detector, producing charge carriers that are moved by the electric field towards the electrodes (Barrientos *et al.*, 2011). The BEGe detector has the highest energy resolution for radiation detection, but is relatively inefficient (Cui and Yang, 2023). Different types of detectors can be designed depending on the impurity, such as n-type: germanium crystals with donor (n-type) impurities or p-type: germanium crystals with acceptor (p-type) impurities (Harkness-Brennan *et al.*, 2014). Figure 2.10 shows the Broad Energy Germanium Gamma Spectrometer system used in this study

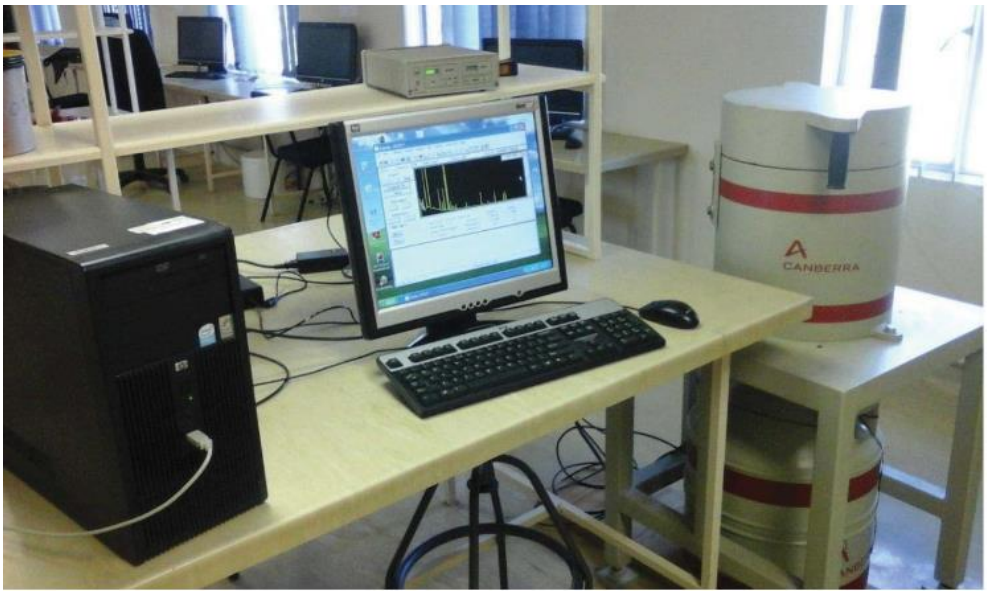

Figure 2. 11: Broad Energy Germanium (BEGe) Gamma Spectrometry system.

Broad Energy Germanium detector configurations can be made in a variety of shapes to suit specific measurement needs. The detector's most common configurations are planar or coaxial (Barrientos *et al.*, 2011). Planar detectors are typically small, with a diameter of a few centimetres. Because of this, the maximum depletion region is limited to less than 1 or 2 cm. This detector is suitable for measuring low-energy gamma radiation (Ravisankar *et al.*, 2014). However, a thicker depletion layer or a larger sensitive volume of the detector required for more general gamma-ray measurements can be achieved by constructing the detector in a different type of cylindrical or coaxial geometry (Harkness-Brennan *et al.*, 2014).

2.6.2 Radioactive Decay Law and Equilibrium

Radioactive decay is random in nature, and it is impossible to predict when a specific atom will decay. However, if numerous atoms are viewed as a single unit, the decay will follow a well-defined statistical pattern known as the radioactive decay law. The decay rate is proportional to the number of radioactive nuclei of a specific type present at any given time, t. The constant of proportionality (λ), also known as the decay constant, is the fraction of atoms that decay in a unit of time, such as a second or a year. It is related to the half-life of a radionuclide, which is the time required for one-half of the original sample to decay (Gruber *et al.*, 2009).

It is more important to know how much radiation is emitted in radiation protection than how many radioactive atoms remain in the sample (Ravisankar *et al.*, 2015). As a result, a quantity known as activity (A) is used to define the number of radioactive material disintegrations that

occur in a unit of time. It is worth noting that the symbols for activity and atomic mass number (A) are the same, as are the symbols for the number of radioactive atoms and the number of neutrons (N). N is the activity of a number of radioactive atoms. As long as there is no new supply of radioactive atoms, the rate of depletion is equal to the rate of activity. According to the law of radioactive equilibrium, the activities of ^{238}U's descendants must be equal to the activity of the ancestor nucleus (Wang *et al.*, 2022). In this study, concentration levels are used to determine the activity for the uranium and thorium examined.

2.7 Significant properties of naturally occurring radioactive materials (NORMs)

NORMs decay to form nuclides, which form a decay chain, resulting in a radioactively stable nuclide (Ntsohi *et al.*, 2021). The ^{238}U decay chain contains several radioactive isotopes before termination with a stable isotope of ^{206}Pb, whereas the ^{235}U decay chain terminates with a stable isotope of ^{207}Pb (Petrosyan and Perikhanyan, 2022, Postar, 2017). Several radioactive isotopes are also present in the ^{232}Th decay chain, before reaching another stable isotope, ^{208}Pb (Long *et al.*, 2012).

Natural potassium isotopes are ^{39}K, ^{40}K, and ^{41}K, with ^{40}K being the only radioactive isotope with a naturally occurring isotopic abundance of 0.0118 %. The beta and electron capture decay modes of ^{40}K to stable ^{40}Ca (89.28%) and ^{40}Ar (10.72%) are followed by the emission of 1460.8 keV gamma rays, which contribute significantly to natural radioactivity (Abbasi *et al.*, 2022). Under most conditions, potassium is soluble and is lost in solution during weathering (Singh *et al.*, 2020). The majority of primordial radionuclide exposure is caused by radon (^{222}Rn) and, to a lesser extent, thoron (^{220}Rn) (Ren *et al.*, 2021, Ravisankar *et al.*, 2015). Radon is a gas that is naturally present in uranium (Gruber *et al.*, 2009, Mudd, 2008). As a result, inhalation of radon gas, and it's by products are the primary sources of radiation exposure in the environment (Almayahi *et al.*, 2012).

CHAPTER 4: MATERIALS AND METHODS

3.1 Introduction

This research was conducted near the Vaal River, which borders the South African provinces of North West, Gauteng, Free State, and Mpumalanga. A total of 27 water samples were collected and prepared for laboratory analysis. This chapter describes the study area and how the samples were collected and prepared for laboratory analysis. Analytical methods, techniques, and processes are also discussed.

3.2 The Study Area

The Vaal River is South Africa's greatest tributary of the Orange River (Wepener *et al.*, 2011). The river's headwaters are in Breyten in Mpumalanga province, some 30 kilometers north of Ermelo and 240 kilometers from the Indian Ocean (Moloi *et al.*, 2020). The climate is subtropical dry savannah, with an annual evaporation rate of 1,300 mm exceeding the annual rainfall rate of 600 mm. River flows and rainfall differ from year to year. The average yearly rainfall is 600 mm. The summer discharge occurs between January and March, and winter discharge occurs between May and July. Both the summer and winter discharges are typically 300 m^3/s per year via storage dams such as the Vaal (2 200 million m^3) and Bloemhof (1 200 million m^3). The winter discharge is 300 m^3/s per year and occurs between May and July (Jury, 2016).

The Vaal River runs west to join the Orange River southwest of Kimberley in the Northern Cape. It is 1,458 kilometers long and divides Mpumalanga, Gauteng, and North West Province on the north bank and the Free State on the south, as shown on figure 3.1 (Du Plessis, 2021, Chokwe *et al.*, 2017). Near Johannesburg, Gauteng, the Vaal River flows west, eventually joining the Orange River and draining into the Atlantic Ocean. After the Orange River (2200 km long) and the Limpopo River (1750 km long), it was established as the principal source of water for the huge Witwatersrand area during the 19th century gold rush (Madzunya *et al.*, 2020, Manyatshe *et al.*, 2017). The Vaal Dam is located on the Vaal River in Deneysville, just south of the border between Gauteng and the Free State (Weideman *et al.*, 2019, Plessl *et al.*, 2019).

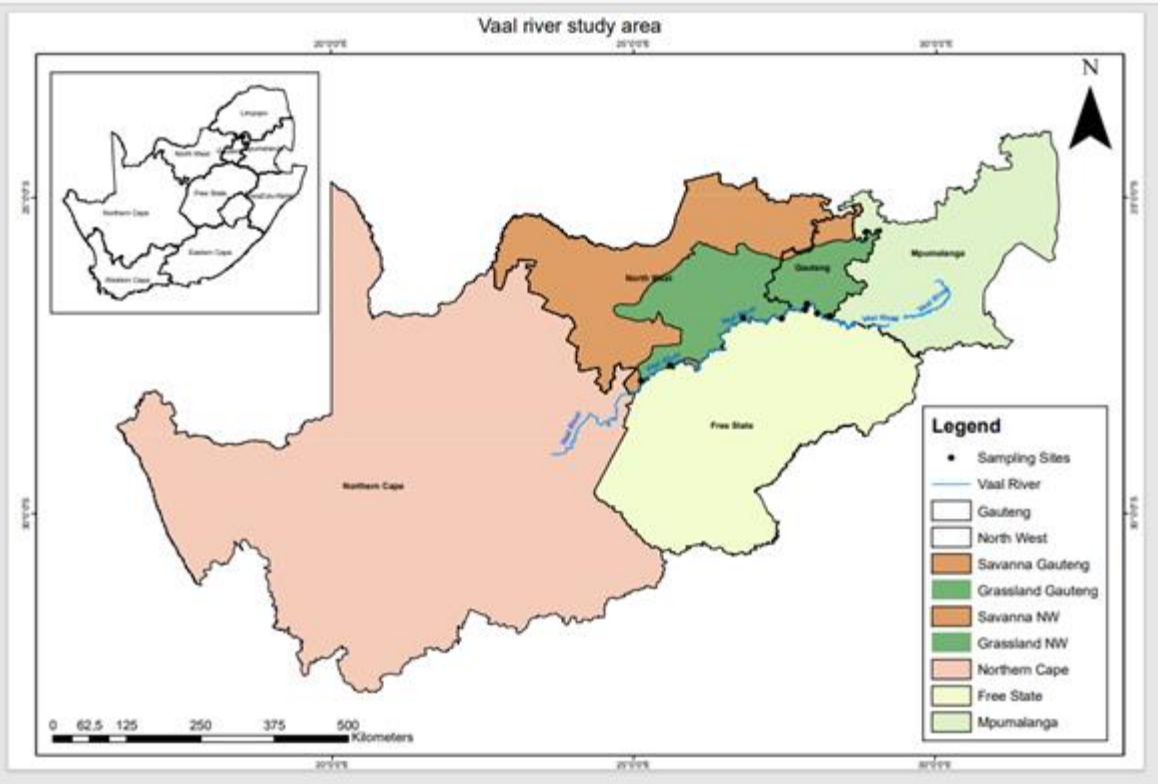

Figure 4.1: Map of the study area.

The Vaal River is one of the rivers that receives a lot of attention regarding its pollution status (Manyatshe *et al.*, 2017, Moloi *et al.*, 2020, van Rensburg *et al.*, 2019, Wepener *et al.*, 2011). The river is said to be South Africa's most polluted (Groffen *et al.*, 2018; Moloi *et al.*, 2020, van Rensburg *et al.*, 2019). It is also well-known for the large amount of contaminants produced by land-use activities (Durand, 2012, Groffen *et al.*, 2018; Moloi *et al.*, 2020). Despite the river's contaminated and polluted image, it is a recreational treasure and plays an important economic role in the country (Manyatshe *et al.*, 2017).

3.2.1 Vaal River activities.

The upstream of the Vaal River is utilized for mining and industrial purposes, such as coal mines, chemical-related industries, as well as urban use and power generation (Plessl *et al.*, 2019). The downstream is largely used for urban needs, although a significant amount is also used for mining and industries, irrigation, and power generation (Manyatshe *et al.*, 2017).

There are many fun ways to enjoy the Vaal River. This could be for enjoyment or to get away from the hustle and bustle of city life (Mararakanye *et al.*, 2022). Beautiful areas like Emerald, Stonehaven, and Vaal River bridge are popular for weekend getaways and leisure. Vaal River provides recreational activities such as boating and fishing (Moloi *et al.*, 2020).

3.3 Sample collection

Water samples were collected from various locations along the Vaal River for three consecutive days from June 23rd to June 25th, 2022. Samples were collected along the riverbanks based on safety and accessibility. The sampling points were chosen based on their proximity to the river and their safety. The samples were collected in and around Gauteng and North West Province, with some samples collected within the borders of the Free State Province. Gauteng Province represented the upper reaches of the river, while North West Province represented the lower reaches. Vanderbijlpark, Emerald, and Stonehaven were the sample sites visited in the Gauteng Province. The majority of the samples were collected in Parys town, which serves as a gateway to both Gauteng and North West provinces. The North West sampling point was near the Scandinavia Drift. Collected samples were geolocated using global positioning system (GPS) indexing as shown in figure 3.2.

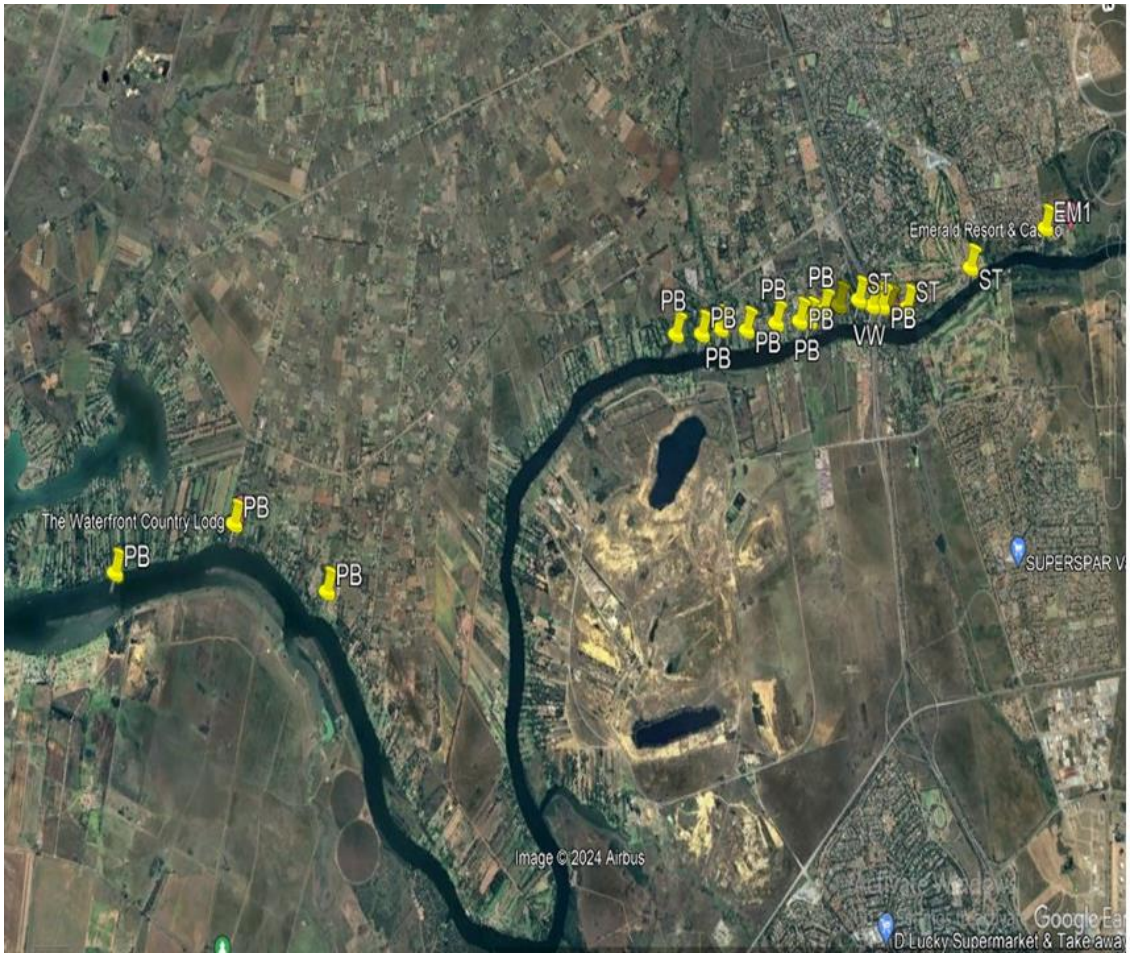

Figure 4.2: Water sample GPS coordinates.

The collected samples were processed at the Environmental Laboratory of the North-West University (Mahikeng campus)'s Centre for Applied Radiation Science and Technology (CARST).

3.3.1 Water sample collection

The majority of the water samples, were collected at the river's public park in Parys, Free State, and Vaal, Gauteng Province. The samples were packaged in 2-litre polythene bottles. To avoid contamination, the bottles were washed prior to use. The bottles were filled to the brim with no gaps to prevent carbon dioxide (CO_2) from being trapped and dissolving in water, which could affect the chemistry. Figure 3.3 shows how water bottles were properly labelled for identification. Because water bottles had to be stored for an extended period of time before analysis, samples were kept at a moderate room temperature. To avoid radionuclide absorption on the bottle walls, 1% of HCI was added to the bottled water sample at a rate of 10 ml per litre immediately after sample collection. For reference purposes, images of samples were taken with a mobile phone and geolocated with a global positioning system (GPS).

Figure 4.3: Water sample collection.

3.4 Sample preparation for laboratory analysis

It is considered during sample preparation that errors can occur if samples are not handled properly. If the errors are not taken seriously, they may have an impact on the results. As a result, each sample was carefully examined to avoid cross-contamination and the loss of heavy metals and radionuclides.

3.4.1 Water sample preparation

Filter paper and a Büchner funnel were used to remove all unnecessary particles from water samples. Water samples were placed in 5 mL plastic bottles and labelled for identification, as shown in figure 3.4. The preparation process was for the ICP- MS analysis.

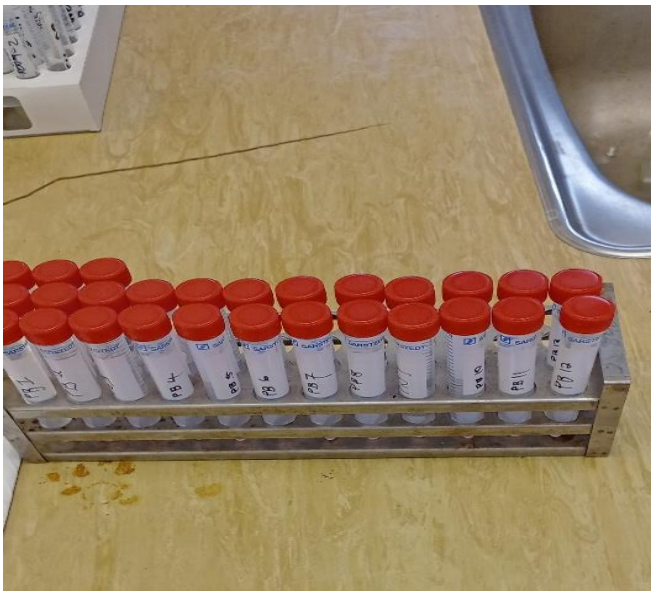

Figure 4.4: Prepared water sample

3.5 Analytic methods

Inductively Coupled Plasma-Mass Spectrometry (ICP -MS) was used to analyse water samples of the Vaal River. The aim of using this method was to analyse the heavy metal concentrations from the water samples collected. In addition to the heavy metals analysed, the K, U and Th analysed and each concentration were converted to activity to assess the radionuclides in water. Ion Chromatography was further used to analyse the cations and anions of the study area.

3.5.1 Sample analysis by Inductively Coupled Plasma-Mass Spectrometry (ICP-MS) method

The water samples were analysed using the Perkin Elmer NexION 2000 ICP-MS method. In this method, the ion beam was focused on the Dual – mode by a Quadrupole ion deflector. The samples were loaded onto the autosampler and the ICP-MS Instrument Syngistix software was used to initialize them. For mass-energy discrimination and interference filtration, the instrument was set to the TotalQuant method in standard mode. For quality control, a multi-element standard calibration solution containing 10 mg/L of Ag, As, Al, Ba, Be, Bi, Cd, Co, Cr, Cs, Cu, Ga, Fe, In, K, Li, Mg, Ni, Na, Pb, Rb, Se, Sr, Ti, U, Zn, V, Th and U was used. For each measurement, the instrument was programmed to perform a blank and a standard check every ten samples.

For this study, the target heavy metals were arsenic (As), lithium (Li), boron (B), Phosphorus (P), lead (Pb), iron (Fe), Manganese (Mn), selenium (Se), cobalt (Co), copper (Cu), nickel (Ni), zinc (Zn), potassium (K), thorium (Th) and uranium (U). The ICP-MS heavy metal concentrations in parts per billion (ppb) were converted to parts per million (ppm) using the following equation:

$$1 \text{ ppb} = 0.001 \text{ ppm} \qquad (3\text{-}1)$$

3.5.2 Ion Chromatography (IC)

The IC method was used for the analysis of cations and anions. The method was chosen due to its quick and accurate analysis of samples. In this method, a set amount of water sample was introduced into the eluent via the switching valve using a sample loop of 10–100 µl. The eluent was pumped continuously through the preconditioned column at a steady flow rate of around 1-2 ml/min. The column, which is packed with uniform resin, is 2-4 mm broad and typically 15 cm long. The anions and cations in the sample were chemically bonded to the resin before being replaced by eluent counter ions of the same charge.

The elution parameters were determined by the resin's ion exchange capacity and the concentration of competing ions in the eluent. The sample would divide into its various components as it passed through the column. The sample components that are weakly bound by the resin move quickly with the flow of the eluent. The components go through the column at different rates and enter the detector at different times. To reduce background noise and

increase detection limits, a suppressor flow-through membrane device was introduced after the column. This was achieved by reducing the eluent's highly conductive strength to a weaker acid. The conductivity detector detects the sample components and generates a chromatogram. By determining the peak area or peak height, one may quantify the concentration by comparing it to recognized standards.

The qualitative description of radionuclide contents in samples and quantitative analysis of their activities required measuring all prepared samples for 12 hours with a gamma-ray spectrometry system equipped with an HPGe detector. To account for the contribution of background radiation, an empty Marinelli beaker was counted for the same time period as the samples, using Genie 2000 software the background was subtracted from the individual spectra of the samples during the analysis.NB: Gamma spectrometry results are not part of this study. Hence they are not reported.

3.6 Calculation of the radionuclides and heavy metals concentrations in water

The concentration of elements in the water (radionuclides and heavy metals) were determined using Inductively Coupled Plasma Mass Spectrometer (ICP-MS) PerkinElmer NexION 2000 using the quant method. To validate the method's accuracy, a 10 ml multi activity calibration standard (Perkin Elmer) with elements was used. The experiment was repeated three times. Blanks and standards were used to test the precision, accuracy, and purity of the reagents used in the analytical procedures.

This study adopted several equations to calculate potential harm of a toxic and harmful substance towards humans over a given period of time. The USEPA (1999) and UNSCEAR (2000) guidelines are used in this study to calculate the human health risks.

3.6.1 Radionuclides in water

Using the conversion factors from the IAEA technical report No1363, the activity concentration (Bq/l) was calculated from the measured concentration (ppm) using the equation (3-2) and (3-4) below (IAEA, 2005):

$$1\% \text{ of } K = 313 \text{ Bq/l} \qquad (3\text{-}2)$$

$$1\text{ppm of } U = 12.35 \text{ Bq/l} \qquad (3\text{-}3)$$

$$1\text{ppm of } Th = 4.06 \text{ Bq/l} \qquad (3\text{-}4)$$

As radiological hazards are determined, the total activity concentration does not provide an exact indication of the radiation hazard associated with the materials. Radium Equivalent (R_{aeq}), Absorbed Dose (D), Annual Effective Dose Equivalent (AEDE), external (H_{ex}) and internal hazard (Hin) index were calculated against the recommended limits by UNSCEAR 2000 of 370 Bq/l, 55 nGy/hr and 1 mSv/yr respectively (Mudd, 2008, UNSCEAR, 2000).

- Radium equivalent activity

Because of the inconsistent distribution of natural radionuclides in the water samples, the actual activity concentration levels of K, U and Th were evaluated using a common radiological index known as radium equivalent activity (Ra_{eq}). It is the most commonly used index for assessing radiation risks (Gruber *et al.*, 2009). Equation (3-5) depicts the radium equivalent activity (Ra_{eq}) calculation.

$$R_{aeq}\,(\text{Bq/l}) = A_u + 1.43A_{Th} + 0.077A_k \qquad (3\text{-}5)$$

The concentrations of U, Th and K in Bq/l are represented by A_u, A_{Th} and A_k. The maximum acceptable value of radium equivalent activity for the general public is 370 Bq/l, which corresponds to an effective dose of 1 mSv/yr. The recommended activity concentration limit by UNSCEAR is 370 Bq/l (UNSCEAR, 2000).

- Absorbed dose rate

The radiation exposures due to radionuclides found in water are of many parameters during the assessment of any radiological hazards. The connection between radioactivity concentrations of natural radionuclides and their exposure is the absorbed dose rate 1 meter above the ground surface. The absorbed dose (D) is the measurement of the amount of energy imparted per unit mass of the irradiated material. A_u, A_{Th} and A_k are the Activity concentrations of U, Th and K respectively. The UNSCEAR recommends a dose limit of 55 nGy/hr as shown in the equation (3-6) (UNSCEAR, 2000). The equation is used to compute the absorbed dose rate by using the average concentrations of U, Th, and K (Bq/l) in the water samples.

$$D(nGy/hr) = 0.462A_U + 0.604A_{Th} + 0.0417A_K \qquad (3\text{-}6)$$

- Annual effective dose equivalent

To quantify the radiological risk directly, annual effective dose equivalent (AEDE) is determined from D rate by using the conversion factor of 0.7 nGy/hr (the measurement for dose rate were converted from nSv/hr to nGy/hr), an outdoor occupancy factor of 0.2, and an

exposure duration per year (8760 hr) as represented in equations (3-6) and (3-7). The total of the tissue-weighted equivalent doses administered to the body's designated organs and tissues is known as the effective dosage. It is mostly used for regulatory purposes to show compliance with exposure dose limitations (Moshupya, 2022). The recommended dose limit by UNSCEAR is 1 mSv/yr (UNSCEAR, 2000).

$$\text{AEDE} = D(nGy/hr) \times 8760 \text{ x } 0.7 \times 0.2 \frac{Sv}{Gy} \times 10^{-6} \qquad (3\text{-}7)$$

The absorbed dose is quantified by the annual effective dose equivalent. This dose is derived from outdoor terrestrial gamma radiation sources and is calculated using two factors: the outdoor occupancy factor and the conversion coefficient from the dose in air to effective dose. The annual effective dose equivalent is estimated using equation 3-7 in conjunction with UNSCEAR's recommended limit of 1 mSv/yr.

Equations 3-8 and 3-9 were used to calculate the hazard indices (AEDE, H_{ex} & H_{in}) of exposure to natural radioactive elements. The maximum of limit is 1 mSv/yr (Almayahi *et al.*, 2012).

$$\text{H}ex = \frac{Au}{370} + \frac{ATh}{259} + \frac{AK}{48100} \qquad (3\text{-}8)$$

$$\text{H}in = \frac{Au}{185} + \frac{ATh}{259} + \frac{AK}{48100} \qquad (3\text{-}9)$$

The external and internal hazard indices due to drinking water were calculated in this study (Abbasi et al., 2022, Ravisankar et al., 2015). According to (Mathuthu *et al.*, 2021) the external and internal hazard index must be less than 1 mSv/yr in order to maintain radiation hazard significance.

3.6.2 Heavy metals in water

In this study, the determination of the carcinogenic or non-carcinogenic health hazards due to ingestion of heavy metals in river water was done using the general exposure pathway equations adopted from (US EPA 1999), for the adult and child age groups (Phalen, 1998). The levels of the exposure of humans to heavy metal was calculated using Equation 3-10, Chronic daily intake (CDI)(mg/kg-day) as:

$$\text{CDI} = \frac{\text{CW} \times \text{IR} \ \text{ABS}_{\text{gi}} \times \text{EF} \times \text{ED}}{\text{BW} \times \text{AT}} \qquad (3\text{-}10)$$

Where CW (mg/L) is the heavy metal concentration in drinking water, IR (L/day) is the ingestion rate – 2.0 L/day used in this study ABS_{gi} (no unit) is the gastrointestinal absorption

factor – 0.001 used in this study (Ismael et al., 2022), EF (days/years) is the exposure frequency – 365 days/year used in this study; ED (years) is the exposure duration – 70 years lifetime (US EPA 1999); BW (kg) is the body weight of the exposed adult person – 70 kg used in this study as average, age specific values (US EPA 1999) and AT (days/year) is the average time, a non-carcinogenic effect period of exposure that is pathway-specific, derived as ED × 365 days/year i.e. 25550 days/year used in this study (USEPA, 1999).

The computed CDI of the heavy metals was used to calculate the hazard quotient, HQ a non-carcinogenic health risks quantity, from Equation 3-13

$$HQ = \frac{CDI}{RfD} \qquad (3\text{-}11)$$

Where RfD (mg/kg/day) is the reference oral-ingested dose adopted from USEPA. The estimated values of HQ less than 1 is within the acceptable level of non-carcinogenic risk, whereas the value with HQ greater than 1 is considered as unacceptable risk with the potential of causing adverse health hazard impact on humans (US EPA 1989). Hazard Index (HI), a non-carcinogenic health risk parameter, is the sum of all the HQs of the individual contaminants, and it provides the estimated values of the whole potential health risks (Uugwanga and Kgabi, 2021). It is determined based on US EPA guidelines using Equation 3-12.

$$HI = \sum_{k=1}^{n} HQ_{HM} \qquad (3\text{-}12)$$

Where HQ_{HM} represents the individual heavy metal's HQ being added up respectively.

The values of HI as computed are being compared to the standard values to ascertain the level or possibility of whether there is a non-carcinogenic health impact on the humans. Hence, for HI value less than 1, imply there is non-carcinogenic health risk whereas for HI values greater than 1, for an exposed person imply there are chances of carcinogenic health risk impact occurring (Moghadam et al., 2024).

3.6.3 Water quality assessment

The heavy metal pollution index (HPI) was used to assess the level of heavy metal pollution in water when compared to their maximum allowable concentrations (MAC). High element concentrations relative to their MAC value indicate poor water quality. An HPI value less than 100, indicates that the water complies with the safety standards and can be consumed; HPI = 100 is the threshold for sage drinking water. An HPI value greater than 100, indicates that the water is not suitable for drinking. Furthermore, the heavy metal evaluation index (HEI) was

used to determine the water quality. An HEI value below 40 indicates a low level of pollution, between 40 and 80 indicates a medium level of pollution, and above 80 indicates a high level of pollution (Agwu et al., 2023, Bawa-Allah, 2023). Equations 3-13 and 3-15 were used:

$$HPI = (C_{Li} \times C_{Mn} \times C_{Fe} x \ldots\ldots\ldots C_N)^{1/N} \quad (3\text{-}13)$$

$$HPI = (C_{Li} \times C_{Mn} \times C_{Fe})^{1/3} \quad (3\text{-}14)$$

$$HEI = \sum \frac{Ci}{CMAC} \quad (3\text{-}15)$$

C_{Li}, C_{Mn}, and C_{Fe} are the heavy metals of interest due to their high concentrations in the water samples of this study (Eq 3-14). The MAC indicates the maximum allowable concentration of heavy metals in mg/l adopted from the WHO 2022 guideline, wherein Li (5 mg/l), Mn (0.05 mg/l m), and Fe (0.3 mg/l) are given. The C*i* is the concentration of heavy metals in the water samples.

HEI less than 1, water acceptable for drinking, HEI = 1 is the threshold, HEI greater than 1, water is unsuitable for drinking (Munkhsuld *et. al.*, 2024).

CHAPTER 5: RESULTS AND DISCUSSIONS

4.1 Presentation of the results

This chapter presents the findings of the study on the water samples collected along the Vaal River. The findings are discussed based on the techniques used. The ICP-MS technique was used, to analyse the radionuclides and heavy metals from the water samples. In this technique, the water samples were analysed for radionuclides such as K, U and Th and heavy metals of interest such as Li, B, P, Ni, Se, Fe, Mn, Pb, Zn and Co. Furthermore, the Ion Chromatography method was used to examine the cations and anions present in the river.

The findings of the study were then computed to assess the potential risks to people. The risk assessment included evaluating potential risks associated with the Vaal River and surrounding communities and it will assist in determining potential mishaps, their likelihood, and consequences, as well as their tolerance. This entails identifying, assessing, and analysing risk factors that indicate the potential of heavy metals to harm people and the environment. The process can also help decision-makers think about different mitigation options.

The exposure risks were calculated based on the concentrations of radionuclides and heavy metals in water. The UNSCEAR, US EPA and WHO recommended limit guideline was used to determine the potential risks of exposure. Previous studies on radionuclide and heavy metals, provided the foundation to this study in terms of guidance on what has been done around the study area.

The chapter presents Results of:

i. NORM radiological risks calculated from the activity concentrations were determined using the (R_{aeq}), absorbed dose (D), annual effective dose equivalent (AEDE) , the external hazard (H_{ex}) and internal Hazard (H_{in}) indexes according to the safe limits of UNSCEAR (UNSCEAR, 2000).
ii. Heavy metal carcinogenic risks to humans calculated from the chronic daily intake (CDI), hazard quotient (HQ), and hazard index (HI) adopted US EPA 1999 guideline. The water quality of the river was determined using the heavy metal pollution index (HPI) and the heavy metal evaluation index (HEI). The permissible limits by WHO, US EPA and UNSCEAR are used in this study to confirm that the concentration levels adhered to the world guideline.

iii. The water types in the study area estimated from the Ion Chromatography (piper diagram) of the cations and anions were then used to determine the water quality.

4.2 Findings on radionuclides and heavy metals

The study focused on radionuclides and heavy metals in the Vaal River in South Africa. The main point of interest was driven by curiosity about the pollution level of the river, the water quality, and the potential impacts on humans. The pollution level and the health hazards posed by radionuclides and heavy metals are assessed using methods discussed in the previous Sections.

4.2.1 Activity concentrations of radionuclides

Water samples taken along the Vaal River were analysed for K, Th and U using ICP-MS. The average, maximum, minimum and standard deviation of the samples were calculated to identify the rate at which the radionuclides are dissolved in the river water. From the calculated concentrations of each sample, the hazard parameters such as R_{aeq}, D, AEDE, H_{ex} and H_{in} were calculated as indicated in Table 4:1.

Table 5.1: K, Th, U activities and the hazard indices in the river water.

Sites	K	Th	U	R_{aeq} (Bq/l)	D (nGy/hr)	AEDE (nGy/hr)	H_{ex}	H_{in}
EM1	467,259	0,021	2,460	38,469	20,634	0,025	0,104	0,111
PB1	359,396	0,002	0,643	28,319	15,285	0,019	0,076	0,078
PB2	428,932	0,005	0,547	33,581	18,142	0,022	0,091	0,092
PB3	429,242	0,003	0,642	33,699	18,198	0,022	0,091	0,093
PB4	392,133	0,004	0,511	30,711	16,590	0,020	0,083	0,084
PB5	412,484	0,003	0,539	32,305	17,452	0,021	0,087	0,089
PB6	432,312	0,002	0,520	33,811	18,269	0,022	0,091	0,093
PB7	423,912	0,004	0,486	33,132	17,904	0,022	0,089	0,091
PB8	432,422	0,002	0,455	33,753	18,243	0,022	0,091	0,092
PB9	402,681	0,039	0,632	31,694	17,108	0,021	0,086	0,087
PB10	412,374	0,004	0,449	32,208	17,406	0,021	0,087	0,088
PB11	401,895	0,002	0,412	31,360	16,950	0,021	0,085	0,086
PB12	427,539	0,002	0,486	33,410	18,054	0,022	0,090	0,092
PB13	439,089	0,002	0,485	34,298	18,536	0,023	0,093	0,094
PB14	446,829	0,006	0,598	35,013	18,913	0,023	0,095	0,096
PB15	362,651	0,003	0,543	28,472	15,376	0,019	0,077	0,078
PB16	392,874	0,003	0,513	30,768	16,622	0,020	0,083	0,084
PV1	441,521	0,006	0,774	34,779	18,772	0,023	0,094	0,096
PV2	454,683	0,006	0,612	35,631	19,247	0,024	0,096	0,098
PV3	444,319	0,005	0,691	34,910	18,850	0,023	0,094	0,096
SD2	386,893	0,013	0,639	30,448	16,437	0,020	0,082	0,084
SD3	430,075	0,009	7,761	40,890	21,525	0,026	0,110	0,131
ST2	444,034	0,006	0,650	34,850	18,820	0,023	0,094	0,096
VW2	243,774	0,737	22,796	42,620	21,155	0,026	0,115	0,177
VW3	463,888	0,013	0,209	35,948	19,449	0,024	0,097	0,098
Av	**414,928 ± 42.000**	**0,036 ± 0.005**	**1,802 ± 0.900**	**33,803 ± 2.500**	**18,158 ± 1.800**	**0,022 ± 0.002**	**0,091 ± 0.001**	**0,096 ± 0.010**
Max	467,259	0,737	22,796	42,620	21,525	0,026	0,115	0,177
Min	243,774	0,002	0,209	28,319	15,285	0,019	0,076	0,078
Std	45,391	0,146	4,617	3,336	1,565	0,002	0,009	0,020

The average radiation hazard of R_{aeq}, D, AEDE, H_{ex} and H_{in} were 33,803 ± 2,500 Bq/l, 18,158 ± 1.800 nGy/hr, 0,222 ± 0.002 nGy/hr, 0,091 ± 0.001 and 0,096 ± 0.010, respectively. These hazard parameters pose no radiological risks to people due to ingestion of the water. This is as a result of lower concentrations when compared to the UNSCEAR limit of 370 Bg/l, 55 nGy/hr, 1 mSv/yr and ratio of 1 for R_{aeq}, D, AEDE, H_{ex} and H_{in} respectively as shown in Table 4:2:

Table 5.2: K, Th, U activities and the UNSCEAR recommended limits.

River water								
	K (Bq/l)	**Th (Bq/l)**	**U (Bq/l)**	**R_{aeq} (Bq/l)**	**D nGy/hr**	**AEDE mSv/yr**	**H_{ex}**	**H_{in}**
Average	414.928	0.036	1.802	33.803	18.158	0.222	0.091	0.096
Max	467.259	0.737	22.796	42.620	21.525	0.026	0.115	0.177
Min	243.774	0.002	0.209	28.319	15.285	0.019	0.076	0.078
Std	45.391	0.146	4.617	3.336	1.565	0.002	0.009	0.020
Recommended limits (UNCEAR, 2000)				**370**	**55**	**1**	**1**	

Table 4:2 presents the average, maximum, minimum and the standard deviation of each K, Th and U in Bq/l for the selected radionuclide analysed using the ICP-MS technique. According to the tabulated concentrations, all the hazard parameters are below the recommended limits of the UNSCEAR 2000 guideline. This proves that the sites where samples were collected pose no radiological risk to people, as of 2023.

Furthermore, the correlation factors were used for the dose rate (D) against the annual effective dose (AEDE) as well as and the radium equivalent (Ra_{eq}) as shown in figure 4.1 Figure 4.2 shows correlation between the D and the AEDE. The results show that the annual absorbed dose (D), is strongly correlated to both Raeq & AEDE.

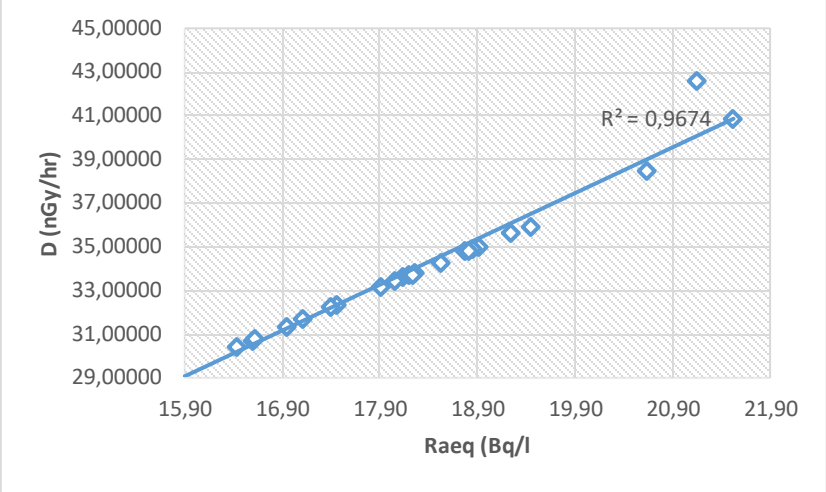

Figure 5.1: Correlation factor D and Raeq

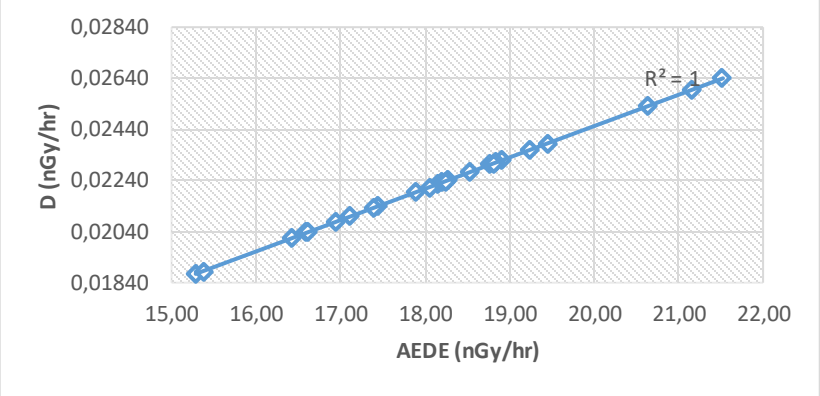

Figure 5.2: Correlation factor D and AEDE

4.2.2 Heavy metal concentrations in water

The sample sites where the Vaal River upstream and downstream water was collected and analysed depicted increased concentrations of elements across the river course. The concentrations of elements increased as the river flows towards the downstream, as shown in Figure 4.3.

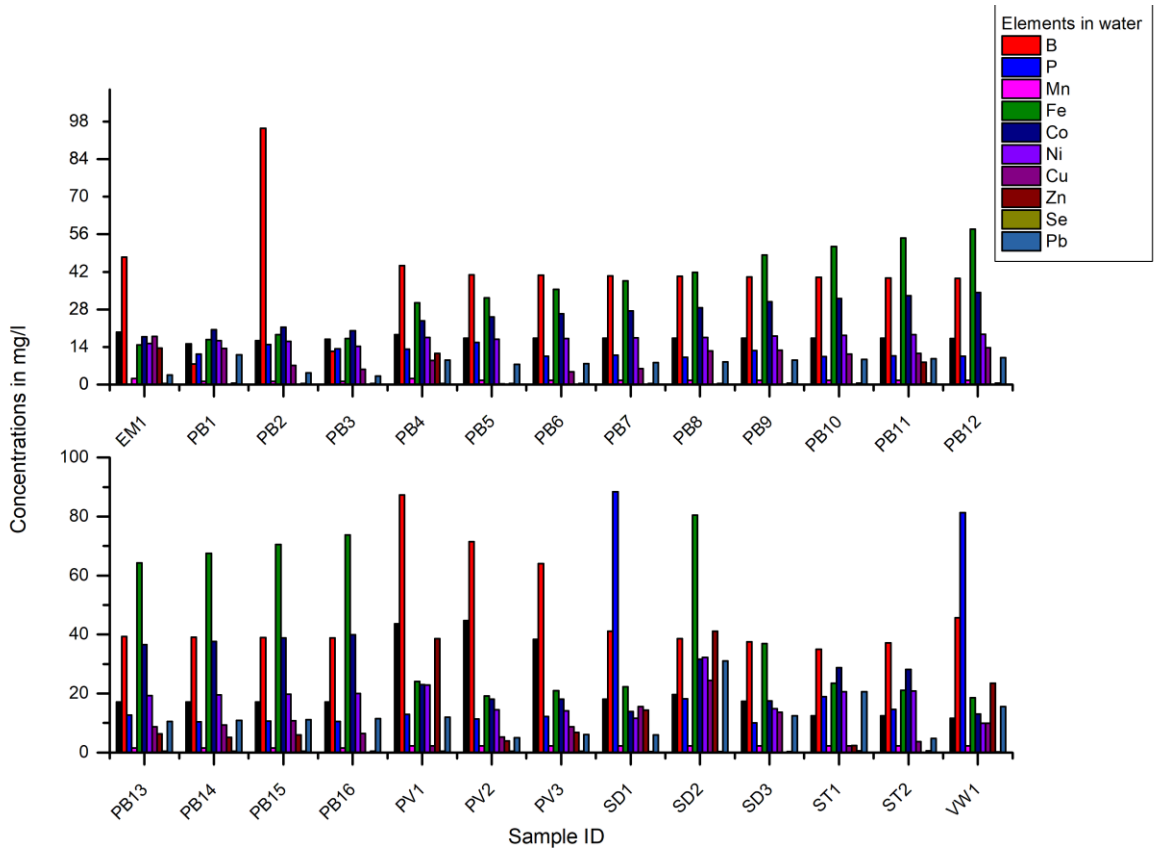

Figure 5.3: Heavy metals in water.

Furthermore, Table 4.3 presents the health risks associated with heavy metal concentration exposure for the water samples collected from the Vaal River. The table compares the average concentrations in the study area to the WHO 2022 limits, while also tabulating the risks posed by excessive and high-dose heavy metal exposure.

Table 5.3: Human health risks due to heavy metal concentration in the river.

Elements	This study Average (ppm)	WHO limit (ppm)	Adverse effects beyond desirable limit
	Water		
Li	0,16	5,00	Appetite loss, vomiting, nausea, abdominal pain and diarrhoea (Avila-Arias *et al.*, 2019).
B	0,03	2,00	Headache, restlessness , renal injury, dermatitis, and indigestion problems (Huo *et al.*, 2022).
P	0,03	0.05	Itchy eyes, joint and muscle pain (Singh *et al.*, 2020).
Mn	4,02	0,05	Skin rashes and poor growth in children (Setia *et al.*, 2023).
Fe	1,34	0,30	Diabetes, heart and liver disease, heart problems (Ugbede *et al.*, 2021).
Co	0,17	0,01	Hearing and vision loss weakness, hypothyroidism and fatigue (Sylvie Désirée *et al.*, 2021).
Ni	0,06	0,10	Lung and nasal cancer, kidney diseases and cardiovascular (Moloi *et al.*, 2020).
Cu	0,05	1,50	Eyes, nose and mouth irritation problem, headache, dizziness and diarrhea (Moloi *et al.*, 2020).
Zn	0,03	5,00	,Stomach pain, headaches and diarrhea (Mokarram *et al.*, 2020).
Se	0,00	0,01	Fever, kidney , nausea as well as liver and heart problems (Plessl *et al.*, 2019).
Pb	0,02	0,05	Anaemia, brain and kidney damage (Ramos *et al.*, 2021, Morales-Silva *et al.*, 2022)

4.2.3 Concentration of heavy metals

The ICP-MS technique measured the elements in ppb and a conversion factor was used. The ppb was converted to ppm. The concentration levels of each element of interest are presented in a table format. To identify how much of an element is dissolved in the river water, the average, maximum, minimum and the standard deviation of the elements were calculated and tabulated in Table 4.4. Among all elements, Mn and Fe are the main elements that are highly dissolved in the river water with an average concentration of 4, 02 mg/l and 1, 34 mg/l respectively. The least dissolved elements in the river water are Li and Se at an average concentration of 0, 16 mg/l and 0.0 mg/l respectively. Table 4.4 presents detailed information of all elements dissolved in the river water.

Table 5.4: Elemental concentrations.

mg/l											
Sites	**Li**	**B**	**P**	**Mn**	**Fe**	**Co**	**Ni**	**Cu**	**Zn**	**Se**	**Pb**
EM1	0,088	0,027	0,025	4,193	0,289	0,218	0,102	0,019	0,013	0,000	0,012
PB1	0,137	0,028	0,012	0,889	0,124	0,114	0,045	0,031	0,007	0,000	0,019
PB2	0,147	0,028	0,011	1,624	0,188	0,132	0,056	0,022	0,008	0,000	0,008
PB3	0,098	0,038	0,015	0,719	0,144	0,142	0,059	0,014	0,006	0,000	0,005
PB4	0,150	0,025	0,020	3,395	0,269	0,149	0,065	0,025	0,011	0,000	0,013
PB5	0,129	0,026	0,012	0,950	0,173	0,117	0,053	0,131	0,019	0,000	0,008
PB6	0,128	0,029	0,016	0,870	0,131	0,122	0,057	0,059	0,015	0,000	0,007
PB7	0,156	0,026	0,022	0,881	0,142	0,126	0,049	0,021	0,006	0,000	0,004
PB8	0,121	0,028	0,012	0,953	0,152	0,088	0,039	0,032	0,008	0,000	0,005
PB9	0,128	0,025	0,014	0,935	0,197	0,106	0,039	0,026	0,009	0,000	0,023
PB10	0,139	0,024	0,022	3,315	0,163	0,112	0,043	0,024	0,009	0,000	0,008
PB11	0,137	0,022	0,008	0,812	0,173	0,097	0,049	0,020	0,007	0,000	0,004
PB12	0,143	0,022	0,013	0,894	0,189	0,139	0,063	0,032	0,013	0,000	0,010
PB13	0,141	0,026	0,013	0,749	0,168	0,132	0,062	0,030	0,012	0,000	0,006
PB14	0,128	0,028	0,019	3,850	0,349	0,138	0,055	0,033	0,011	0,000	0,014
PB15	0,124	0,022	0,020	3,244	0,273	0,127	0,062	0,037	0,012	0,000	0,012
PB16	0,111	0,034	0,012	4,421	0,252	0,132	0,050	0,019	0,008	0,000	0,009
PV1	0,323	0,070	0,015	5,328	0,272	0,138	0,092	0,095	0,043	0,000	0,023
PV2	0,306	0,061	0,011	4,030	0,280	0,148	0,070	0,020	0,010	0,000	0,009
PV3	0,258	0,054	0,024	4,688	0,248	0,148	0,070	0,035	0,013	0,000	0,011
SD-2	0,136	0,028	0,032	11,004	0,843	0,242	0,125	0,090	0,040	0,000	0,063
SD-3	0,112	0,031	0,015	5,381	0,435	0,138	0,069	0,053	0,018	0,000	0,026
ST2	0,107	0,023	0,019	3,772	0,255	0,275	0,108	0,015	0,007	0,000	0,010
VW-2	0,479	0,042	0,306	30,123	27,457	0,835	0,000	0,313	0,328	0,052	0,241
VW-3	0,078	0,034	0,015	3,419	0,238	0,104	0,051	0,039	0,029	0,000	0,030
Av	0,160	0,030	0,030	4,020	1,340	0,170	0,060	0,050	0,030	0,00	0,020
Max	0,480	0,070	0,310	30,120	27,460	0,840	0,120	0,310	0,330	0,05	0,240
Min	0,080	0,020	0,010	0,720	0,120	0,090	0,00	0,010	0,010	0,00	0,000
Std	0,090	0,010	0,060	5,920	5,440	0,150	0,030	0,060	0,060	0,010	0,050

Throughout the sample sites, Se presented no dissolved concentrations in water except at the VW2. This can be due to the insolubility of Se in water. According to WHO guidelines, the limit of Se in drinking water should not exceed 0.01 mg/l, therefore the calculated average concentration proves to be safe for people where there is possibility of ingestion. The same site (VW2) presented high dissolved concentration of Fe at 27.457mg/l. This concentration is higher than the recommended limit of 0.3 mg/l. Fe as a metal is not soluble in water, but Fe as a salt is soluble in water. The probability is that the Fe found in VW2 is a Fe salt, based on its concentration level.

The high concentrations can be due to industrial effluent because the site is closer to the industries. Iron and manganese are metallic elements that are commonly found in water and are essentially required in small amount by all living organisms. According to WHO, the required permit for Fe, Mn are 0.3 mg/l and 0.05 mg/l respectively. The study limit of Fe and Mn, 1.34 mg/l and 4.02 mg/l respectively, are of high dissolved concentration in water which may result in human health risks. Based on the findings of the study, it is significant to note that heavy metals can pass into the aquatic environment, groundwater and plants, reaching humans and animals (Zhou *et al.*, 2020b). These metals can be easily transferred from one place to another due to their persistency in the environment (Khan *et al.*, 2022, Rani *et al.*, 2022). They can also be ingested by humans through food and water (Edokpayi *et al.*, 2022). Their toxic level depends on the dose rate and the type of metal (Klubi *et al.*, 2020). Some heavy metals such as Se, even in small amounts, can cause illness in the human body and affect body organs (Klubi *et al.*, 2020). Major sources of these elements were agricultural sludge and fertilizers, municipal sewage and the nearby mining.

In addition to the average dissolved concentrations of each element. This study measured the potential harm of the element of interest to the people where there is exposure over a period of time. The study used an adult of 70 years at 70kg body weight and a child at 15 years (15 kg) body weight for 365 days per year. The human health risks in relation to cancer were determined using the chronic daily intake (CDI), hazard quotient (HQ), and hazard indices (HI) adopted from the US EPA 1989 guideline. Table 4:5 presents detailed information concerning the risks to children.

Table 5.5: Child health risks indices for children.

Heavy metal	CW mg/l	CDI mg/kg/day (US EPA 2011)	RfD mg/kg/day (US EPA 2011)	HQ	Risk value (15 yrs)
Li	0.2	6.39E+02	0.02	3.20E+04	3,2
Mn	4.2	1.68E+04	0.14	1.20E+05	1,2
Fe	1.2	4.80E+03	0.30	1.60E+04	1,6
Ni	0.06	2.40E+02	0.02	1.20E+04	1,2
Cu	0.05	2.00E+02	0.04	5.00E+03	0,5
Zn	0.03	1.20E+02	0.30	4.00E+02	4,0
Pb	0.02	7.99E+01	0.14	5.71E+02	5,7
Hazard Index (HI)	2.7				

The chronic daily intake (CDI) and the reference oral-ingested dose (RfD) presented in Table 4:5 and 4:6 are the permissible ingestion limits set by the US EPA 2011 guideline. According to the findings of the water samples collected from the river, the river water has HQ greater than 1 in all samples. The HI, which is the sum of the HQ, is also greater than 1. The HI values greater than 1 implies carcinogenic health risks for a person exposed to the pollutant. The calculated risks for each element are greater than 1. This implies that the elemental concentration are of carcinogenic risks to a child aged 15 at a body weight of 15 kg. The calculated elemental concentration of Cu are less than 1 at the ratio of 0.5 as a result, the dissolved concentration levels of Cu pose non-carcinogenic risk.

Table 4:5 of the human health indices presents the information concerning the children at age 70 years. The risks thereof are greater than 1. According to the findings of this study, the sample sites where water samples were collected are of carcinogenic risks to an adult aged 70, at a body weight of 70kg. The HI which is the sum of HQ also present the ratio greater than 1, which implies carcinogenic risks when there is exposure to a pollutant.

Table 5.6: Adult health indices.

Heavy metal	CW mg/l	CDI mg/kg/day (US EPA 2011)	RfD mg/kg/day (US EPA 2011)	HQ	Risk value (70 yrs)
Li	0.2	2.98E+03	0.02	3.20E+04	1.5
Mn	4.2	7.83E+04	0.14	1.20E+05	5.5
Fe	1.2	2.40E+04	0.30	1.60E+04	7.5
Ni	0.06	1.12E+03	0.02	1.20E+04	5.6
Cu	0.05	9.33E+02	0.04	5.00E+03	2.3
Zn	0.03	5.60E+02	0.30	4.00E+02	1.9
Pb	0.02	3.73E+02	0.14	5.71E+02	2.7
Hazard Index (HI)	1.2				

4.2.4 Water quality assessment

The Vaal River water was analysed using heavy metal pollution Index (MPI) which evaluates the pollution concentration level in water. The heavy metal evaluation index (HEI) was also used to assess the water quality with regard to the dissolved concentration of elements in water. The maximum allowable concentration (MAC) used in this study to determine the water quality was adopted from the US EPA. Table 4. 7 presents the HPI and HEI for the elements of interest for this study.

Table 4.7: MPI and HEI for the elements of interest for this study (mg/l).

SAMPLE ID	Li	Mn	Fe	MPI
EM-1	0,088	4,193	0,289	0,036
PB-1	0,137	0,889	0,124	0,005
PB-2	0,147	1,624	0,188	0,015
PB-3	0,098	0,719	0,144	0,003
PB-4	0,150	3,395	0,269	0,046
PB-5	0,129	0,950	0,173	0,007
PB-6	0,128	0,870	0,131	0,005
PB-7	0,156	0,881	0,142	0,007
PB-8	0,121	0,953	0,152	0,006
PB-9	0,128	0,935	0,197	0,008
PB-10	0,139	3,315	0,163	0,025
PB-11	0,137	0,812	0,173	0,006
PB-12	0,143	0,894	0,189	0,008
PB-13	0,141	0,749	0,168	0,006
PB-14	0,128	3,850	0,349	0,057
PB-15	0,124	3,244	0,273	0,037
PB-16	0,111	4,421	0,252	0,041
PV-1	0,323	5,328	0,272	0,156
PV-2	0,306	4,030	0,280	0,115
PV-3	0,258	4,688	0,248	0,100
SD-2	0,136	11,004	0,843	0,422
SD-3	0,112	5,381	0,435	0,087
ST-2	0,107	3,772	0,255	0,034
VW-2	0,479	30,123	27,457	132058,258
VW-3	0,078	3,419	0,238	0,021
HEI	**0,03**	**80,35**	**4,45**	

The calculated MPI for each element per site is shown in Table 4.7. The MAC for Li is 5 mg/l, and for Fe & Mn it is 0.3 m/l and 0.05 mg/l respectively, as per the WHO guideline. Sample VW-2 present high HPI = 132058.258, (mainly from Mn & Fe contributions), while all other

samples are less than the WHO limit of 1. This implies poor water quality concerning the dissolved concentration of Fe and Mn in water.

Mn presents higher HEI = 80.35 for all sites. This indicates poor water quality due to the dissolved concentration of Mn in the river water, and hence the Vaal River water does not comply with the safety standards. There is a high level of Mn metal pollution

The HEI of the Li and Fe are below the value of 40, this indicates low pollution level. From the HPI & HEI values of Fe & Mn, we conclude that Mn is the major pollutant of the water in the Vaal River. This could be due to human activities such as industrial discharges, since the site is located closer to industries and mines. According to the findings of the study, the Vaal River is not suitable for use due to the level of heavy metal (Mn & Fe) pollution. Exposure to pollutants may result in human health risks.

The study's findings were based on accessible sites such as Emerald Resort (EM1), which represented the Vaal River's upstream, and Scandinavia Drift (SD1 and 2), which represented the river's downstream. The upstream, like the downstream, was mostly used for entertainment and relaxation. The PB represented the Vaal River's public bridge and crossed the river both upstream and downstream. The public bridge was extensively used for pleasure and picnics. In short, the public extensively used the Vaal River.

Previous research did not focus on heavy metals in water. Kamunda *et al.* (2017) focused on the dangers associated with heavy metals in the Witwatersrand's Gauteng Gold Mining Basin, which was the upstream of the Vaal River for this study. Fewer elements, such as Ni, Pb, and Zn, were found in high amounts in the study by Kamunda *et al.* (2017) when compared to the world average limit.

Manyatshe *et al.* (2017), on the other hand, investigated the amounts of pollutants in water in the North West Province, namely around Potchefstroom. In this current study, Potchefstroom represented the Vaal River's downstream. Manyatshe *et al.* (2017) focused primarily on the water quality of the Vaal River, however decreased Fe concentrations were projected. In this study, the majority of the heavy metal elements, such asc, Li, B, P, Ni, Se, Fe, Mn, Pb, Zn and Co were analysed for concentrations. Table 4.8 contains detailed information on previous studies mentioned as well as the study to date.

Table 5.8: Statistical summary of heavy metal levels in the study area.

Elements	Kamunda *et al* (2017) Average soil concentrations (mg/kg)	Manyatshe *et al* (2017) Average water concentrations (mg/l)	This study (2023) Average water concentrations (mg/l)
Ni	115,9	N/A	0,06
Zn	68,0	N/A	0,03
Pb	50,79	N/A	0,02
Co	4,7	N/A	0,17
Fe	N/A	11.3	1,34
P	N/A	1.3	0,03
B	N/A	N/A	0,03
Mn	N/A	N/A	4,02
Li	N/A	N/A	0,16
Se	N/A	N/A	0,00

4.3 Findings on the cations and anions using Ion Chromatography.

In this study, the piper phases in Figure 4.4 were used to interpret the results found in Figure 4.5.

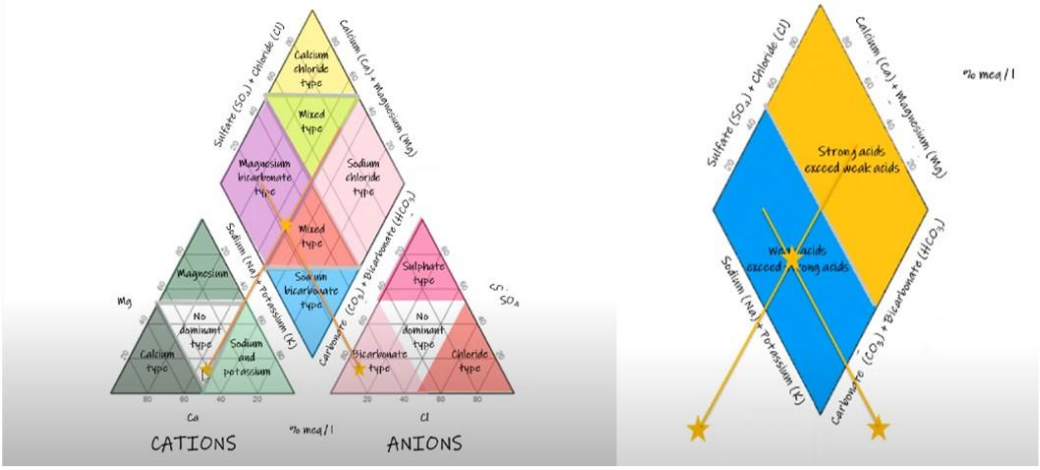

Figure 5.4: Piper Phases.
https://www.youtube.com/watch?v=ha6x3uJVJ_Y&list=RDCMUCGAgjGCEH2SDl12M91D-10Q

In this study, the cations measured are calcium (Ca^{2+}), sodium (Na^{+}), magnesium (Mg^{2+}), and potassium (K^{+}), with average concentrations of 34.4, 58.9, 13.8, and 6.3 mg/l, respectively. In addition to the cations, the anions included sulphate (SO_4^{2-}), phosphate (PO_4^{3}), and nitrite (NO_2), with an average concentration of 87.5, 0.7, and 0.1 mg/l. The total cations were calculated as the sum of calcium (Ca^{2+}), sodium (Na^{+}), magnesium (Mg^{+}), and potassium (K^{+}). The anions were calculated as sulphate (SO_4^{2-}), phosphate (PO_4^{3-}), and nitrite (NO_2). The samples had an ion balance in the 1% range, indicating that the ion analysed were not acceptable. The values obtained from the water samples in conjunction with the piper diagram present the mixed water types. Furthermore, a trilinear diagram showing water types was used as shown in Figure 4.5. This confirms that the acidity of the water is due to sulphuric acid from the Acid Mine Drainage. The acid is used for processing (extracting minerals e.g. U, etc) from the Ores.

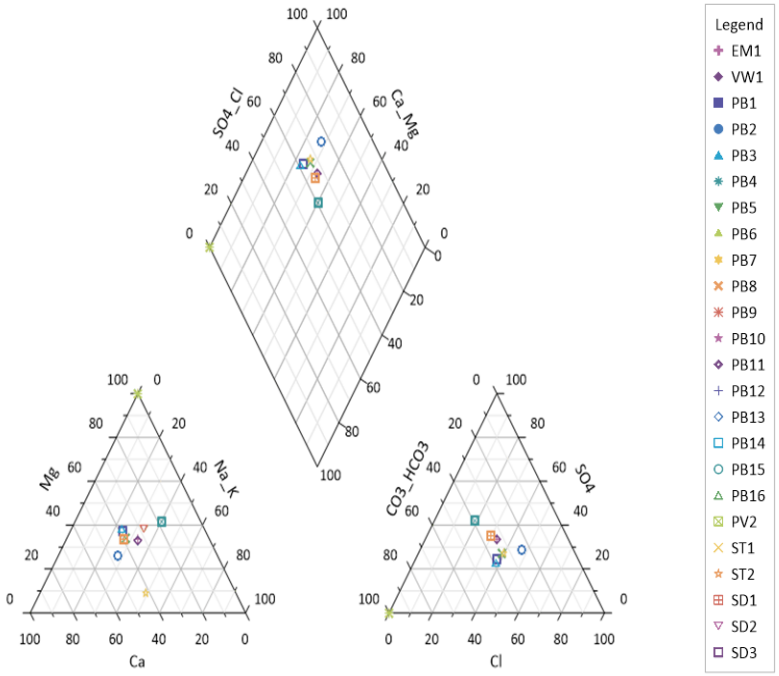

Figure 5.5: Cation and anions piper diagram.

The ion balance for each sample site was calculated as the total concentrations of the cations minus the total concentrations of anions, divided by the total concentrations of ions dissolved. The recommended concentration limit for Na^+, and SO_4^{2-} are 200 and 500 mg/l respectively (DNR, 2009).

The water types of the samples studied were depicted using a trilinear (piper) diagram. Sulphate-chloride, sodium-potassium, bicarbonate, chloride, calcium, and magnesium were among the water types. As demonstrated in Figure 4.5 of a piper diagram, the cations and anions presented a non-dominant form of water, while the combination of cations and anions presented a mixed type of water.

In this study, the cations and anions were measured to identify the ionic composition of the water, which is used to characterize and describe the chemical quality of the river water. This was done to categorize ionic types based on the majority of dissolved cations and anions in mg/l. The analysed samples in this study are Ca-Mg- SO_4, illustrating the dominance of mixed types, where more than one type of element dominates in the samples examined. The cations and anions showed no dominant type; hence, the water types could not be categorised.

4.4 Challenges regarding the sustainability of the Vaal River for future water supply

The Vaal River is one of the South African rivers that is facing multiple anthropogenic challenges. According to several studies, the Vaal River is polluted beyond acceptable levels, with pollution sources including discharge from nearby mines, agricultural run-off, and sewage sludge (Kamunda, 2017, Manyatshe *et al.*, 2017, Moshupya, 2022). In this study, the samples analysed were collected along the Vaal River, for analysis of radionuclides, heavy metals and water quality. According to the findings of the study, the hazard parameters of radionuclides posed no radiological risk when compared to the safety standard recommended by the UNSCEAR and the US EPA guidelines. In relation to the heavy metal elements, the findings presented Vaal River as not safe for public use due to the high concentrations of Fe and Mn. In addition to the human health risks, the study assessed the water quality. Based on the findings, it is concluded that the Vaal River is not of good quality due to increased level of Mn and Fe in water when compared to the permitted values.

In support to the current study, Marara and Palamuleni, (2019) conducted research on the Klip River, which is an important tributary of the Vaal River. The authors contend that heavy metal contamination of rivers is caused by anthropogenic activities such as mining, agriculture, wastewater, and industrial effluents. The mining activity is argued as a major concern in river water pollution, posing potential risks to humans, animals, and the ecosystem at large.

In 2017, Kamunda *et al* presented high concentrations of heavy metals such as Zn and Ni in soil, as well as uranium at (574.3 Bq/kg). In 2022, Moshupya *et al* also presented potential radiological risks due to elevated concentration of Uranium at (827.9 Bq/l). Based on the studies conducted, it is of great concern to observe elevated concentrations of pollution within and around the Vaal River.

South Africa's National Nuclear Regulator (NNR) conducted an independent assessment of the radiological and heavy metal impacts of mine water discharges on local communities around the Klerksdorp and Potchefstroom of the Vaal River (NNR, 2007). The study's findings confirmed uranium as a toxic chemical that posed a risk to water users in the catchment. The study discovered that the catchment's mean heavy metal concentration levels exceeded the regulated concentration levels (NNR, 2007). The South African Water Research Commission (WRC) also reported in their March 2006 scientific research report (Boer *et al.*, 2006) that the measured uranium concentrations of many fluvial sediments in the water catchment areas

(WCA), including those of off-mine properties, exceeded the NNR regulatory limit (NNR, 2007).

Toxic heavy metals in water were found in high concentrations in this study, which exceeded the WHO guidelines. As a result of the findings reported from the previous studies and this study, the sustainability of the Vaal River is questionable. The river's ability to meet human needs while also allowing the natural system to deliver important ecosystem services to humans may be jeopardized. The desirable conditions in which rivers meet human demands without jeopardizing the natural system's stability are of great significance. According to the conclusions of earlier studies and this study, the river's sustainability may not satisfy the needs of future generations unless the challenges are addressed and resolved. As a result, a conceptual management plan is recommended as a solution to the Vaal River's difficulties in this study.

CHAPTER 6: CONCLUSION AND RECOMMENDATIONS

5.1 Conclusions

The study intended to investigate the concentration levels of the radioactive and heavy metals of the Vaal River, to evaluate the human health risks and the water quality of the river. The ICP-MS technique was used due to its lower interference, and quick multi-element analysis benefits for environmental samples.

The average radiation hazard of R_{aeq}, D, AEDE, H_{ex} and H_{in} complies with the safety limit of UNSCEAR. As a result, pose no radiological risks to human. This is justified by using an adult of 70 years and a child of 15 years for a period of a year. This also implies that the sites where samples were collected have lower concentrations of radioactive materials.

In relation to the heavy metal concentration levels of the study, Mn and Fe presented higher concentration. These elements are known to be common and highly dissolved in water, however the higher concentrations could be due to the human activities of industrial and agricultural effluent. The HI of the study presented a ratio greater than 1, which implies a carcinogenic risk toward humans. The elevated concentrations are possibly due to the nearby mine effluent, especially taking into consideration that the river is situated nearby the mine. There is also the possibility of discharges from the local municipalities, and agricultural run-off since the space is extensively used for various uses such as industrial and municipal activities.

The water quality of the river was also determined using the water quality indices such as the HPI and HEI. The average concentration of the HPI in relation to the Mn increased is greater than the value of 1, as a result the Vaal River does not comply with the safety standards. The HEI also a ratio greater than 80 which shows high level of pollution of heavy metals in the river. The water quality for this study, in relation to analyses of cations and anions, presented water types as Ca-Mg-SO_4.

Based on the findings of prior studies and this study, the site is not safe for public use until more investigation is carried out. As a result, additional monitoring and regulatory control measures are required to safeguard the safety of all residents in these areas.

5.2 Recommendations

More research is required to better understand the origins of contamination along the Vaal River. Surface, subterranean, erosion, run-off evaluation, and the development of pilot treatment methods such as covering mining wastes with vegetation and introducing natural plants that might assist in limiting water pollution could all be examples of pollution interventions.

Sites along the Vaal River that were not included in this analysis can be investigated further for heavy metal and radioactive contamination. Membrane technology applications can be investigated, and the results can be used to address the difficulties of pollution in the Vaal River.

Additionally, a conceptual management plan with ideas for improving the state of the river's problems can be used to manage the river. This study proposes a conceptual management plan with ideas and a timeline for the management of the river. Management of the Vaal River will contribute to sufficient and adequate water quality for drinking, sanitation, food production, energy generation, and recreation, as well as the maintenance of healthy and dependent ecosystem services. The fundamental goal of the conceptual management plan is to improve the Vaal River through planning, monitoring, collaborations, and social and leadership abilities. All participants acting in harmony is a frequent strategy for maintaining water quality. The concept is built on a bottom-up decision-making process in which local communities can participate and have their voices heard.

Figure 5.1 proposes a partnership and collaboration among stakeholders, specifically industry, government, community, and environmental organizations. These collaborations must ensure that planning methods include evaluation and monitoring efforts that effectively manage rivers, are inclusive, and involve local communities. Sustainability can be achieved in this way by taking a holistic approach that considers ecological, social, and economic needs. Figure 5.1 depicts how the approach should be ongoing and involve all stakeholders.

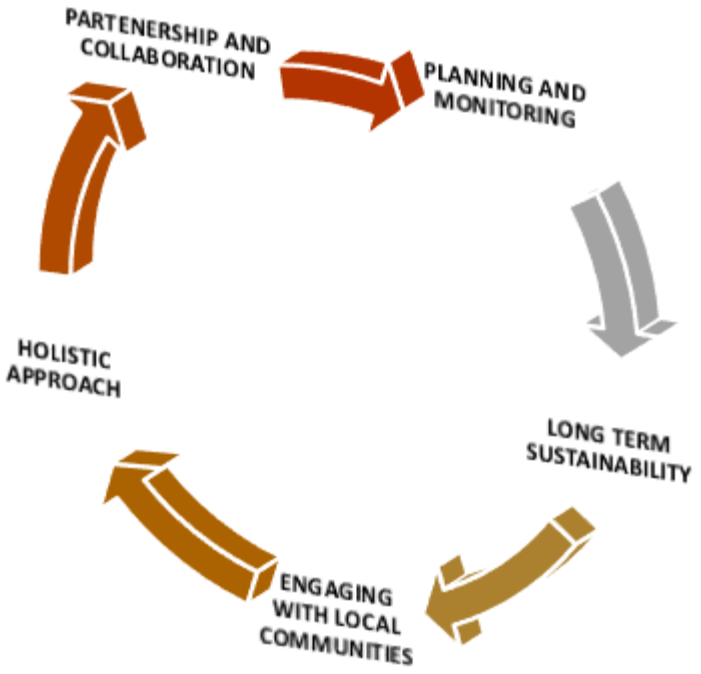

Figure 6.1: Schematic diagram of the conceptual management plan.

This conceptual management plan's purpose is to direct river use and monitoring while also addressing the interaction between rivers and human behaviour by promoting river amenity and social value. The purpose is also to promote collaborative practice, in which new ways of thinking arise from the expertise and experience of different river users. Active water bodies such as the local municipality, the Department of Water and Sanitation (DWS), the South African Local Government Association (SALGA), the Rand Water Board, and the Water Research Commission can all share information. The purpose of sharing information is to ensure inclusivity and understanding of Vaal River developments.

Researchers operating in the Vaal River should ensure that their research data is easily accessible to Policy makers. A central database should be created where all data gathered through studies or reports by active bodies using the river and testing its water is easily accessible. Furthermore, a workable website for all interested and active people working on Vaal River initiatives should provide a platform for them to register themselves so that everyone is informed of what is going on along the river.

People and rivers share an unbreakable bond of depending on the river for water, pleasure and relaxation. Anthropogenic activities such as mining effluent and, agricultural run-off, sewage and municipal waste that contribute to river pollution will not abate as a result of people

engaging with rivers unless they are addressed in a way that is inclusive of people, fair, transparent, and involves people. When it comes to river difficulties, most people tend to separate themselves from the problem, thinking that the water comes from the tap, causing people to forget where the water comes from. It is now vital to increase awareness in order to reconnect people and waterways. Some leisure activities, such as fishing and boating, are already popular, all communities inside and surrounding rivers must be included to avoid waste discharges into rivers.

5.2.1 Conceptual management plan timeline

This study proposes a timeline for the proposed action. According to this study, an awareness meeting should be held in February 2025 to raise awareness to the local communities nearby the Vaal River. This accommodates the users of the Emerald Resort, Stonehaven and other sites that are of private space. Once the awareness is raised, the planning meeting on the way forward concerning the cleaning and management of the river can potentially take place around May 2024. This is where the issues of the river get addressed by various users. All stakeholders of the river need to be part of the planning. This includes the local municipalities, agricultural and mining representatives, Rand Water Board as well as the local users.

Once the planning is well addressed, the way forward can be conducted. This will include the cleaning and maintenance of the river by all users involved. During this meeting, a date can be set where all users can clean the river. Since we know that the main problem is heavy metals and radionuclides in the water, the river water will need to be cleaned using the biological method and the maintenance plan should be created to ensure that all the hard work is not wasted. The maintenance plan should include when, where and how to clean the river before and after the cleaning process.

Furthermore, the report on heavy metal safety management, as well as uranium and thorium, should be employed. Appropriate guidelines should be prepared to guide industry, municipalities, and mining corporations, based on the opinions of knowledgeable individuals such as (researchers, Water Research Groups, Rand Water Board, Department of Water and Sanitation). This will ensure the safe handling of materials containing uranium and thorium, among other elements. The guideline must first identify the pollutants of the Vaal River and then give proposed solutions. The advice will help to improve safety and reduce unnecessary radiation exposure. Finally, a central database where essential information can be saved must

be established. The timeline shown in Table 5.1 elaborates the actions to guide the developments of the management plan.

Table 5.1 Conceptual management plan timeline

Proposed action	***February 2025***	***May 2025***	***August 2025***	***November 2025***
Awareness	√√√			
Planning meeting		√√√		
Way forward meeting			√√√	
Creation of central database			√√√	
Creation of central website for interested and affected parties				√√√

REFERENCES

ABBASI, A., ALGETHAMI, M., BAWAZEER, O. & ZAKALY, H. M. H. 2022. Distribution of natural and anthropogenic radionuclides and associated radiation indices in the Southwestern coastline of Caspian Sea. *Marine Pollution Bulletin,* 178**,** 113593.

ABUSULTAN, A. A. M., WOOD, J. A., SAINIO, T., KEMPERMAN, A. J. B. & VAN DER MEER, W. G. J. 2023. Ion exchange resin – Bipolar membrane electrodialysis hybrid process for reverse osmosis permeate Remineralization: Preparative ion exchange chromatography for Ca2+ and Mg2+ recovery. *Separation and Purification Technology,* 317**,** 123799.

AGWU, E. J., ODANWU, S. E., EZEWUDO, B. I., ODO, G. E., NZEI, J. I., IHEANACHO, S. C. & ISLAM, M. S. 2023. Assessment of water quality status using heavy metal pollution indices: A case from Eha-Amufu catchment area of Ebonyi River, Nigeria. *Acta Ecologica Sinica,* 43**,** 989-1000.

AICHINGER, H., DIERKER, J., JOITE-BARFUß, S. & SÄBEL, M. 2012. Interaction of Photons with Matter. *Radiation Exposure and Image Quality in X-Ray Diagnostic Radiology*. Springer.

AJIBADE, F. O., ADELODUN, B., LASISI, K. H., FADARE, O. O., AJIBADE, T. F., NWOGWU, N. A., SULAYMON, I. D., UGYA, A. Y., WANG, H. C. & WANG, A. 2021. Chapter 25 - Environmental pollution and their socioeconomic impacts. *In:* KUMAR, A., SINGH, V. K., SINGH, P. & MISHRA, V. K. (eds.) *Microbe Mediated Remediation of Environmental Contaminants*. Woodhead Publishing.

ALMAYAHI, B. A., TAJUDDIN, A. A. & JAAFAR, M. S. 2012. Radiation hazard indices of soil and water samples in Northern Malaysian Peninsula. *Applied Radiation and Isotopes,* 70**,** 2652-2660.

ARAI, Y., WATANABE, S., HASEGAWA, K., OKAMURA, N., WATANABE, M., TAKEDA, K., FUKUMOTO, H., AGOU, T., HAGURA, N. & TSUKAHARA, T. 2023. Evaluation of the remaining spent extraction solvent in vermiculite after leaching tests via PIXE analysis. *Nuclear Instruments and Methods in Physics Research Section B: Beam Interactions with Materials and Atoms,* 542**,** 206-213.

ARAL, H. & VECCHIO-SADUS, A. 2011. Lithium: Environmental Pollution and Health Effects. *In:* NRIAGU, J. (ed.) *Encyclopedia of Environmental Health (Second Edition)*. Oxford: Elsevier.

ASHOK, C., VISHWAKARMA, S. R. & DEO, M. N. 2019. Fourier transform spectroscopic investigations of atomic bismuth (209Bi I) in the spectral region from IR to UV (2500−40,000 cm−1). *Journal of Quantitative Spectroscopy and Radiative Transfer,* 229**,** 60-70.

ASHRAF, S., RIZVI, N. B., RASOOL, A., MAHMUD, T., HUANG, G. G. & ZULFAJRI, M. 2020. Evaluation of heavy metal ions in the groundwater samples from selected automobile workshop areas in northern Pakistan. *Groundwater for Sustainable Development,* 11**,** 100428.

ATANGANA, E. & OBERHOLSTER, P. J. 2021. Using heavy metal pollution indices to assess water quality of surface and groundwater on catchment levels in South Africa. *Journal of African Earth Sciences,* 182**,** 104254.

AVILA-ARIAS, H., NIES, L. F., GRAY, M. B. & TURCO, R. F. 2019. Impacts of molybdenum-, nickel-, and lithium- oxide nanomaterials on soil activity and microbial community structure. *Science of The Total Environment,* 652**,** 202-211.

BAMANA, G., MILLER, J. D., YOUNG, S. L. & DUNN, J. B. 2021. Addressing the social life cycle inventory analysis data gap: Insights from a case study of cobalt mining in the Democratic Republic of the Congo. *One Earth,* 4**,** 1704-1714.

BARRIENTOS, D., BOSTON, A. J., BOSTON, H. C., QUINTANA, B., SAGRADO, I. C., UNSWORTH, C., MOON, S. & CRESSWELL, J. R. 2011. Characterisation of a Broad Energy Germanium (BEGe) detector. *Nuclear Instruments and Methods in Physics Research Section A: Accelerators, Spectrometers, Detectors and Associated Equipment,* 648**,** S228-S231.

BAWA-ALLAH, K. A. 2023. Assessment of heavy metal pollution in Nigerian surface freshwaters and sediment: A meta-analysis using ecological and human health risk indices. *Journal of Contaminant Hydrology,* 256**,** 104199.

BEZUIDENHOUT, J. 2021. Estimating indoor radon concentrations based on the uranium content of geological units in South Africa. *Journal of Environmental Radioactivity,* 234**,** 106647.

BIRD, G., BREWER, P. A., MACKLIN, M. G., SERBAN, M., BALTEANU, D. & DRIGA, B. 2005. Heavy metal contamination in the Arieş river catchment, western Romania: Implications for development of the Roşia Montană gold deposit. *Journal of Geochemical Exploration,* 86**,** 26-48.

BLOCH, R. & OWUSU, G. 2012. Linkages in Ghana's gold mining industry: Challenging the enclave thesis. *Resources Policy,* 37**,** 434-442.

BOLAN, N., HOANG, S. A., TANVEER, M., WANG, L., BOLAN, S., SOORIYAKUMAR, P., ROBINSON, B., WIJESEKARA, H., WIJESOORIYA, M., KEERTHANAN, S., VITHANAGE, M., MARKERT, B., FRÄNZLE, S., WÜNSCHMANN, S., SARKAR, B., VINU, A., KIRKHAM, M. B., SIDDIQUE, K. H. M. & RINKLEBE, J. 2021. From mine to mind and mobiles – Lithium contamination and its risk management. *Environmental Pollution,* 290**,** 118067.

BURRITT, R. L. & CHRIST, K. L. 2018. Water risk in mining: Analysis of the Samarco dam failure. *Journal of Cleaner Production,* 178**,** 196-205.

BUZETZKY, D., KÓNYA, J., KOVÁCS, E. M., BALLA, A. K., KREMPER, R., KÁTAI, J. & NAGY, N. M. 2023. Analysis of phosphorus forms on different soil types using heterogeneous isotope exchange reaction. *Soil and Tillage Research,* 225**,** 105557.

CHAVES, C., PEREIRA, E., FERREIRA, P. & GUERNER DIAS, A. 2021. Concerns about lithium extraction: A review and application for Portugal☆. *The Extractive Industries and Society,* 8**,** 100928.

CHOKWE, T. B. & OKONKWO, J. O. 2019. Occurrence, distribution and ecological risk assessment of organophosphorus flame retardants and plasticizers in sediment samples along the Vaal River catchment, South Africa. *Emerging Contaminants,* 5**,** 173-178.

CHOKWE, T. B., OKONKWO, J. O. & NWAMADI, M. S. 2017. Occurrence and distribution of tetrabromobisphenol A and its derivative in river sediments from Vaal River Catchment, South Africa. *Emerging Contaminants,* 3**,** 121-126.

CHOUDHURY, T. R., FERDOUS, J., HAQUE, M. M., RAHMAN, M. M., QURAISHI, S. B. & RAHMAN, M. S. 2022. Assessment of heavy metals and radionuclides in groundwater and associated human health risk appraisal in the vicinity of Rooppur nuclear power plant, Bangladesh. *Journal of Contaminant Hydrology,* 251**,** 104072.

CLAASSENS, L., DAHMS, S., VAN VUREN, J. H. J. & GREENFIELD, R. 2016. Artificial mussels as indicators of metal pollution in freshwater systems: A field evaluation in the Koekemoer Spruit, South Africa. *Ecological Indicators,* 60**,** 940-946.

CÓRDOVA-LIZAMA, A., CARRERA-FIGUEIRAS, C., PALACIOS, A., CASTRO-OLIVERA, P. M. & RUIZ-ESPINOZA, J. 2022. Improving hydrogen production from the anaerobic digestion of waste activated sludge: Effects of cobalt and iron zero valent nanoparticles. *International Journal of Hydrogen Energy,* 47**,** 30074-30084.

CUI, T. & YANG, Y. 2023. Yield calculation for delayed gamma-ray neutron activation analysis. *Nuclear Instruments and Methods in Physics Research Section A: Accelerators, Spectrometers, Detectors and Associated Equipment,* 1054**,** 168380.

CUI, T., YU, M. & YANG, Y. 2023. The epithermal neutron activation analysis of mineral ores driven by an electron linear accelerator-based photoneutron source. *Nuclear Instruments and Methods in Physics Research Section A: Accelerators, Spectrometers, Detectors and Associated Equipment,* 1048**,** 167878.

DA SILVA, A. P. V., SILVA, A. O., LIMA, F. R. D. D., BENEDET, L., FRANCO, A. D. J., SOUZA, J. K. D., RIBEIRO JÚNIOR, A. C., BATISTA, É. R., INDA, A. V., CURI, N., GUILHERME, L. R. G. & CARNEIRO, M. A. C. 2022. Potentially toxic elements in iron mine tailings: Effects of reducing soil pH on available concentrations of toxic elements. *Environmental Research,* 215**,** 114321.

DAN, S. F., UDOH, E. C. & WANG, Q. 2022. Contamination and ecological risk assessment of heavy metals, and relationship with organic matter sources in surface sediments of the Cross River Estuary and nearshore areas. *Journal of Hazardous Materials,* 438**,** 129531.

DAS, R., MANDAL, B., SARKAR, D., PRADHAN, A. K., DATTA, A., PADHAN, D., SETH, A., KUMAR, R., DE, N., MISHRA, V. N., POLARA, K. B., SHARMA, S., THAKUR, N. P., KACHROO, D., RAY, M., SHARMA, A., PATEL, K. P., GARNAYAK, L. M. & NARKHEDE, W. N. 2019. Boron availability in soils and its nutrition of crops under long-term fertility experiments in India. *Geoderma,* 351**,** 116-129.

DAVIES, T. C. & MUNDALAMO, H. R. 2010. Environmental health impacts of dispersed mineralisation in South Africa. *Journal of African Earth Sciences,* 58**,** 652-666.

DEHDASHTI, B., AMIN, M. M. & CHAVOSHANI, A. 2020. Chapter 6 - Other trace elements (heavy metals) and chemicals in aquatic environments. *In:* CHAVOSHANI, A., HASHEMI, M., MEHDI AMIN, M. & AMETA, S. C. (eds.) *Micropollutants and Challenges.* Elsevier.

DEVI, S. S. & MEHENDALE, H. M. 2014. National Center for Environmental Health-ATSDR. *In:* WEXLER, P. (ed.) *Encyclopedia of Toxicology (Third Edition).* Oxford: Academic Press.

DÍAZ-MORALES, D. M., ERASMUS, J. H., BOSCH, S., NACHEV, M., SMIT, N. J., ZIMMERMANN, S., WEPENER, V. & SURES, B. 2021. Metal contamination and

toxicity of soils and river sediments from the world's largest platinum mining area. *Environmental Pollution,* 286**,** 117284.

DNR, I. 2009. Water Quality Standards Review: Cloride, Sulfate and Total Dissolved Solids. Iowa Department of Natural Resources

DU PLESSIS, A. 2021. Necessity of making water smart for proactive informed decisive actions: A case study of the upper vaal catchment, South Africa. *Environmental Challenges,* 4**,** 100100.

DURAND, J. F. 2012. The impact of gold mining on the Witwatersrand on the rivers and karst system of Gauteng and North West Province, South Africa. *Journal of African Earth Sciences,* 68**,** 24-43.

DUTTA, D., GOEL, S. & KUMAR, S. 2022. Health risk assessment for exposure to heavy metals in soils in and around E-waste dumping site. *Journal of Environmental Chemical Engineering,* 10**,** 107269.

EDOKPAYI, J. N., NKHUMELENI, M., ENITAN-FOLAMI, A. M. & OLANIYI, F. C. 2022. Water quality assessment and potential ecological risk of trace metals in sediments of some selected rivers in Vhembe district, South Africa. *Physics and Chemistry of the Earth, Parts A/B/C***,** 103111.

FRANCHI, S., DI MARCO, V. & TOSATO, M. 2022. Bismuth chelation for targeted alpha therapy: Current state of the art. *Nuclear Medicine and Biology,* 114-115**,** 168-188.

GANI, K. M., HLONGWA, N., ABUNAMA, T., KUMARI, S. & BUX, F. 2021. Emerging contaminants in South African water environment- a critical review of their occurrence, sources and ecotoxicological risks. *Chemosphere,* 269**,** 128737.

GENTHE, B., KAPWATA, T., LE ROUX, W., CHAMIER, J. & WRIGHT, C. Y. 2018. The reach of human health risks associated with metals/metalloids in water and vegetables along a contaminated river catchment: South Africa and Mozambique. *Chemosphere,* 199**,** 1-9.

GROFFEN, T., WEPENER, V., MALHERBE, W. & BERVOETS, L. 2018. Distribution of perfluorinated compounds (PFASs) in the aquatic environment of the industrially polluted Vaal River, South Africa. *Science of The Total Environment,* 627**,** 1334-1344.

GRUBER, V., MARINGER, F. J. & LANDSTETTER, C. 2009. Radon and other natural radionuclides in drinking water in Austria: Measurement and assessment. *Applied Radiation and Isotopes,* 67**,** 913-917.

HANTO, J., SCHROTH, A., KRAWIELICKI, L., OEI, P.-Y. & BURTON, J. 2022. South Africa's energy transition – Unraveling its political economy. *Energy for Sustainable Development,* 69**,** 164-178.

HARKNESS-BRENNAN, L. J., JUDSON, D. S., BOSTON, A. J., BOSTON, H. C., COLOSIMO, S. J., CRESSWELL, J. R., NOLAN, P. J., ADEKOLA, A. S., COLARESI, J., COCKS, J. F. C. & MUELLER, W. F. 2014. An experimental characterisation of a Broad Energy Germanium detector. *Nuclear Instruments and Methods in Physics Research Section A: Accelerators, Spectrometers, Detectors and Associated Equipment,* 760**,** 28-39.

HATAM, E. G., PELICON, P., PUNZON-QUIJORNA, E., KELEMEN, M., VAVPETIČ, P. & PONGRAC, P. 2023. Application of four-segments annular Silicon drift detector for

3-D surface topography reconstruction by micro-PIXE. *Nuclear Instruments and Methods in Physics Research Section B: Beam Interactions with Materials and Atoms,* 541**,** 205-215.

HILSON, G. & CLIFFORD, M. J. 2010. Small-scale gold mining, the environment and human health: an introduction to the Ghana case. *International Journal of Environment and Pollution,* 41**,** 185-194.

HUANG, Z., SUN, M., ZHENG, Y., HAN, Y., LIU, H. & SHEN, J. 2023. A micro sample pretreatment technique combined with ion chromatography and its application in the determination of polyvinyl chloride. *Journal of Chromatography A,* 1690**,** 463778.

HUNG, N. Q., HAI, V. H. & NOMACHI, M. 2017. Investigation of cosmic-ray induced background of Germanium gamma spectrometer using GEANT4 simulation. *Applied Radiation and Isotopes,* 121**,** 87-90.

HUO, J., SONG, B., RIAZ, M., SONG, X., LI, J., LIU, H., HUANG, W., JIA, Q. & WU, W. 2022. High boron stress leads to sugar beet (Beta vulgaris L.) toxicity by disrupting photosystem II. *Ecotoxicology and Environmental Safety,* 248**,** 114295.

ISMAEL, M., MOKHTAR, A., ADIL, H., LI, X. & LÜ, X. 2022. Appraisal of heavy metals exposure risks via water pathway by using a combination pollution indices approaches, and the associated potential health hazards on population, Red Sea State, Sudan. *Physics and Chemistry of the Earth, Parts A/B/C,* 127**,** 103153.

ISSAH, M. & UMEJESI, I. 2018. Risks and vulnerability in uranium mining: A synthesis of local perspectives in the Great Karoo region of South Africa. *The Extractive Industries and Society,* 5**,** 284-293.

JIBIRI, N. N. & OKEYODE, I. C. 2012. Evaluation of radiological hazards in the sediments of Ogun river, South-Western Nigeria. *Radiation Physics and Chemistry,* 81**,** 103-112.

JOHNSON, B. L. 1995. ATSDR's information databases to support human health risk assessment of hazardous substances. *Toxicology Letters,* 79**,** 11-16.

JOYCE, M. 2018. Chapter 15 - Radioactive Waste Management and Disposal. *In:* JOYCE, M. (ed.) *Nuclear Engineering.* Butterworth-Heinemann.

JURY, M. R. 2016. Climate Influences on Vaal River 42.

KAMUNDA, C. 2017. Health Risk Assessment of Heavy Metals in Soils from Witwatersrand Gold Mining Basin, South Africa.

KATHREN, R. L. 1998. NORM sources and their origins. *Applied Radiation and Isotopes,* 49**,** 149-168.

KHALEEQ, A., AHMED, M., HUMA, R., MUJTABA, A., NOOR, S., REHMAN, R., SHEIKH, T. A., QAMAR, S., IQBAL, D. N., ALHARTHY, R. D. & HAMEED, A. 2022. Evaluation of trace and heavy metals in different varieties of sauces to characterize their impact on human health. *Journal of Food Composition and Analysis,* 114**,** 104789.

KHAN, K., YOUNAS, M., SHARIF, H. M. A., WANG, C., YASEEN, M., CAO, X., ZHOU, Y., IBRAHIM, S. M., YVETTE, B. & LU, Y. 2022. Heavy metals contamination, potential pathways and risks along the Indus Drainage System of Pakistan. *Science of The Total Environment,* 809**,** 151994.

KHUMALO, N. & MATHUTHU, M. 2018. Determination of trace elements and lanthanide (REE) signatures in uranium mine products in South Africa by means of inductively coupled plasma mass spectrometry. *Journal of Geochemical Exploration,* 186**,** 235-242.

KLUBI, E., ABRIL, J. M., MANTERO, J., GARCÍA-TENORIO, R. & NYARKO, E. 2020. Environmental radioactivity and trace metals in surficial sediments from estuarine systems in Ghana (Equatorial Africa), impacted by artisanal gold-mining. *Journal of Environmental Radioactivity,* 218**,** 106260.

LANDSBERGER, S. 2022. Discovery of neutron activation analysis. *Applied Radiation and Isotopes,* 189**,** 110422.

LI, D., HUANG, W. & HUANG, R. 2023. Analysis of environmental pollutants using ion chromatography coupled with mass spectrometry: A review. *Journal of Hazardous Materials,* 458**,** 131952.

LI, D. & LIU, S. 2019. Chapter 10 - Drinking Water Detection. *In:* LI, D. & LIU, S. (eds.) *Water Quality Monitoring and Management*. Academic Press.

LI, Z., WANG, J. & DING, M. 2022. A review on optimization methods for nuclear reactor fuel reloading analysis. *Nuclear Engineering and Design,* 397**,** 111950.

LIN, L. & LIU, X. 2022. Estimation of total iron in soil using a water-absorption-peak-based color reconstructing machine (WCRM) method. *Biosystems Engineering,* 220**,** 233-242.

LINDMAN, Å., RANÄNGEN, H. & KAUPPILA, O. 2020. Guiding corporate social responsibility practice for social license to operate: A Nordic mining perspective. *The Extractive Industries and Society,* 7**,** 892-907.

LITTLE, A. J., SIVARAJAH, B., FRENDO, C., SPRAGUE, D. D., SMOL, J. P. & VERMAIRE, J. C. 2020. The impacts of century-old, arsenic-rich mine tailings on multi-trophic level biological assemblages in lakes from Cobalt (Ontario, Canada). *Science of The Total Environment,* 709**,** 136212.

LIU, Q., LI, Y., LIU, S., GAO, W., SHEN, J., ZHANG, G., XU, H., ZHU, Z., GE, T. & WU, J. 2022. Anaerobic primed CO2 and CH4 in paddy soil are driven by Fe reduction and stimulated by biochar. *Science of The Total Environment,* 808**,** 151911.

LIU, Y., WANG, P., GOJENKO, B., YU, J., WEI, L., LUO, D. & XIAO, T. 2021. A review of water pollution arising from agriculture and mining activities in Central Asia: Facts, causes and effects. *Environmental Pollution,* 291**,** 118209.

MA, M., WANG, R., XU, L., XU, M. & LIU, S. 2020. Emerging health risks and underlying toxicological mechanisms of uranium contamination: Lessons from the past two decades. *Environment International,* 145**,** 106107.

MADZUNYA, D., DUDU, V. P., MATHUTHU, M. & MANJORO, M. 2020. Radiological health risk assessment of drinking water and soil dust from Gauteng and North West Provinces, in South Africa. *Heliyon,* 6**,** e03392.

MAKUBALO, S. S. & DIAMOND, R. E. 2020. Hydrochemical evolution of high uranium, fluoride and nitrate groundwaters of Namakwaland, South Africa. *Journal of African Earth Sciences,* 172**,** 104002.

MANYATSHE, A., FOSSO-KANKEU, E., VAN DER BERG, D., LEMMER, N., WAANDERS, F. & TUTU, H. 2017. Dispersion of inorganic contaminants in surface water in the vicinity of Potchefstroom. *Physics and Chemistry of the Earth, Parts A/B/C,* 100**,** 86-93.

MARARA, T. & PALAMULENI, L. G. 2019. An environmental risk assessment of the Klip river using water quality indices. *Physics and Chemistry of the Earth, Parts A/B/C,* 114**,** 102799.

MARARAKANYE, N., LE ROUX, J. J. & FRANKE, A. C. 2022. Long-term water quality assessments under changing land use in a large semi-arid catchment in South Africa. *Science of The Total Environment,* 818**,** 151670.

MASAC, J., MACHYNAK, L., LOVIC, J., BEINROHR, E. & CACHO, F. 2021. On-line electrochemical preconcentration and electrochemical hydride generation for determination of antimony by high-resolution continuum source atomic absorption spectrometry. *Talanta,* 223**,** 121767.

MASOK, F. B., MASITENG, P. L., MAVUNDA, R. D., MALEKA, P. P. & WINKLER, H. 2018. Determination of uranium and thorium concentration and gross alpha and beta activity measurement in top soil samples from Richards Bay, South Africa. *Journal of Radiation Research and Applied Sciences,* 11**,** 305-310.

MATHUTHU, M., UUSHONA, V. & INDONGO, V. 2021. Radiological safety of groundwater around a uranium mine in Namibia. *Physics and Chemistry of the Earth, Parts A/B/C,* 122**,** 102915.

MEERT, C. A., PANTER, A. P., JINIA, A. J., MACDONALD, A. T., CLARKE, S. D., PIERSON, B. D. & POZZI, S. A. 2022. High-fidelity photoneutron detection via neutron activation analysis. *Nuclear Instruments and Methods in Physics Research Section A: Accelerators, Spectrometers, Detectors and Associated Equipment,* 1040**,** 167116.

MHLONGO, S. P., MATIVENGA, P. T. & MARNEWICK, A. 2018. Water quality in a mining and water-stressed region. *Journal of Cleaner Production,* 171**,** 446-456.

MOGHADAM, S. M., PAYANDEH, K., KOUSHAFAR, A., GOOSHEH, M. & ROUZBAHANI, M. M. 2024. Human health risk assessment and carcinogenicity due to exposure to potentially toxic elements on soil pollution in Southwest Iran. *Clinical Epidemiology and Global Health,* 25**,** 101492.

MOKARRAM, M., SABER, A. & SHEYKHI, V. 2020. Effects of heavy metal contamination on river water quality due to release of industrial effluents. *Journal of Cleaner Production,* 277**,** 123380.

MOLOI, M., OGBEIDE, O. & VOUA OTOMO, P. 2020. Probabilistic health risk assessment of heavy metals at wastewater discharge points within the Vaal River Basin, South Africa. *International Journal of Hygiene and Environmental Health,* 224**,** 113421.

MORALES-SILVA, T., SILVA, B. C. & FARIA, L. D. B. 2022. Soil contamination with permissible levels of lead negatively affects the community of plant-associated insects: A case of study with kale. *Environmental Pollution,* 304**,** 119143.

MOSHUPYA, P. M. M., S.C.; ABIYE, T.A.; KORIR, I.; NHLEKO, S.; MKHOSI, M 2022. In Situ Determination of Radioactivity Levels and Radiological Doses in and around the Gold Mine Tailing Dams, Gauteng Province, South Africa. *Minerals,* 12.

MUDD, G. M. 2008. Radon releases from Australian uranium mining and milling projects: assessing the UNSCEAR approach. *Journal of Environmental Radioactivity,* 99**,** 288-315.

NANGEELIL, K., DIMPFL, P., MAMTIMIN, M., HUANG, S. & SUN, Z. 2023. Preliminary study on forgery identification of Hetian Jade with Instrumental Neutron Activation Analysis. *Applied Radiation and Isotopes,* 191**,** 110535.

NNR 2007. Safety assessment of radiation hazards to members of the public from NORM activities. *In:* P MAMPE, P. H., W SPEELMAN, J PULE AND F RATSHILI (ed.).

NOVIKAU, R. & LUJANIENE, G. 2022. Adsorption behaviour of pollutants: Heavy metals, radionuclides, organic pollutants, on clays and their minerals (raw, modified and treated): A review. *Journal of Environmental Management,* 309**,** 114685.

NTSOHI, L., USMAN, I., MAVUNDA, R. & KUREBA, O. 2021. Characterization of uranium in soil samples from a prospective uranium mining in Serule, Botswana for nuclear forensic application. *Journal of Radiation Research and Applied Sciences,* 14**,** 23-33.

OJEKUNLE, O. Z., RASAKI, A., TAIWO, A. M., ADEGOKE, K. A., BALOGUN, M. A., OJEKUNLE, O. O., ANUMAH, A. O., IBRAHIM, A. O. & ADEYEMI, A. 2022. Health risk assessment of heavy metals in drinking water leaching through improperly managed dumpsite waste in Kurata, Ijoko, Sango area of Ogun State, Nigeria. *Groundwater for Sustainable Development,* 18**,** 100792.

ORDÓÑEZ, J., GALLARDO, S., ORTIZ, J. & MARTORELL, S. 2019. Coincidence summing correction factors for 238U and 232Th decay series using the Monte Carlo method. *Radiation Physics and Chemistry,* 155**,** 244-247.

PAULL, B. & MICHALSKI, R. 2019. Ion Exchange | Ion Chromatography Principles and Applications☆. *In:* WORSFOLD, P., POOLE, C., TOWNSHEND, A. & MIRÓ, M. (eds.) *Encyclopedia of Analytical Science (Third Edition).* Oxford: Academic Press.

PETROSYAN, V. & PERIKHANYAN, Y. 2022. Assessment of possible risks on human health by estimation of annual effective doses associated with radon in drinking water. *Applied Radiation and Isotopes,* 189**,** 110406.

PHALEN, R. F. 1998. Uncertainties relating to the health effects of particulate air pollution: The US EPA's particle standard. *Toxicology Letters,* 96-97**,** 263-267.

PLESSL, C., GILBERT, B. M., SIGMUND, M. F., THEINER, S., AVENANT-OLDEWAGE, A., KEPPLER, B. K. & JIRSA, F. 2019. Mercury, silver, selenium and other trace elements in three cyprinid fish species from the Vaal Dam, South Africa, including implications for fish consumers. *Science of The Total Environment,* 659**,** 1158-1167.

POSTAR, S. 2017. The half-lives of African uranium: A historical review. *The Extractive Industries and Society,* 4**,** 398-409.

POURCELOT, L., MASSON, O., BEGUIN-LEPRIEUR, M., BOULET, B., CAGNAT, X., DE VISMES-OTT, A., HABIBI, A., JAEGLER, H., WAMPACH, C., DIAS VARELA, D., FLEURY, S., TREILLE, F., HENNEQUET, P., MÉTIVIER, J.-M., COSSONNET, C., RAYNAL, J. C. & NOACK, Y. 2021. Using the activity of naturally occurring radionuclides to identify the contribution of the Al industry to the atmosphere and plants. *Applied Geochemistry,* 131**,** 105033.

PRZYBYLA, J., MCCLURE, P. R., ZACCARIA, K. J. & POHL, H. R. 2021. Chemical interactions and mixtures in public health risk assessment: An analysis of ATSDR's interaction profile database. *Regulatory Toxicology and Pharmacology,* 125**,** 104981.

RAMOS, Q., ARMIENTA, M. A., AGUAYO, A. & CRUZ, O. 2021. Evaluation of the interactions of arsenic (As), boron (B), and lead (Pb) from geothermal production wells with agricultural soils. *Ecotoxicology and Environmental Safety,* 211**,** 111843.

RANI, L., SRIVASTAV, A. L., KAUSHAL, J., GREWAL, AJMER S. & MADHAV, S. 2022. Chapter 3 - Heavy metal contamination in the river ecosystem. *In:* MADHAV, S., KANHAIYA, S., SRIVASTAV, A., SINGH, V. & SINGH, P. (eds.) *Ecological Significance of River Ecosystems.* Elsevier.

RAVISANKAR, R., CHANDRAMOHAN, J., CHANDRASEKARAN, A., PRINCE PRAKASH JEBAKUMAR, J., VIJAYALAKSHMI, I., VIJAYAGOPAL, P. & VENKATRAMAN, B. 2015. Assessments of radioactivity concentration of natural radionuclides and radiological hazard indices in sediment samples from the East coast of Tamilnadu, India with statistical approach. *Marine Pollution Bulletin,* 97**,** 419-430.

RAVISANKAR, R., SIVAKUMAR, S., CHANDRASEKARAN, A., PRINCE PRAKASH JEBAKUMAR, J., VIJAYALAKSHMI, I., VIJAYAGOPAL, P. & VENKATRAMAN, B. 2014. Spatial distribution of gamma radioactivity levels and radiological hazard indices in the East Coastal sediments of Tamilnadu, India with statistical approach. *Radiation Physics and Chemistry,* 103**,** 89-98.

REN, X., WANG, J., ZHONG, Q., BI, Q., ZHU, R. & DU, J. 2021. Radionuclide and trace metal accumulation in a variety of mosses used as bioindicators for atmospheric deposition. *Science of The Total Environment,* 797**,** 149224.

ROBINSON, B. H., YALAMANCHALI, R., REISER, R. & DICKINSON, N. M. 2018. Lithium as an emerging environmental contaminant: Mobility in the soil-plant system. *Chemosphere,* 197**,** 1-6.

RUNCIE, J. W. & LARKUM, A. W. D. 2001. Estimating Internal Phosphorus Pools in Macroalgae Using Radioactive Phosphorus and Trichloroacetic Acid Extracts. *Analytical Biochemistry,* 297**,** 191-192.

RUTGERS VAN DER LOEFF, M. M. 2019. Uranium-Thorium Decay Series in the Oceans: Overview☆. *In:* COCHRAN, J. K., BOKUNIEWICZ, H. J. & YAGER, P. L. (eds.) *Encyclopedia of Ocean Sciences (Third Edition).* Oxford: Academic Press.

SAAD, D., NDLOVU, M., RAMAREMISA, G. & TUTU, H. 2022. Microplastics in freshwater environment: the first evaluation in sediment of the Vaal River, South Africa. *Heliyon,* 8**,** e11118.

SALGADO, W. L., DE FREITAS DAM, R. S., XAVIER DA SILVA, A. & SALGADO, C. M. 2023. Void fraction prediction using prompt gamma neutron activation analysis and artificial intelligence. *Radiation Physics and Chemistry,* 213**,** 111212.

SATYANARAYANA, A. V. S., JAGANNADHA RAO, M. & GURU, T. V. S. P. V. S. 2022. Analytical result of charnockites by PIXE and its comparison with other analytical technique XRF. *Materials Today: Proceedings,* 62**,** 4351-4354.

SAYAM, A. S. M., ISLAM, M. A., ALI, M. R., HOSSAIN KHAN, M. M. & ISHRAK, M. F. 2023. Neutron activation analysis of sediments of the Padma River adjacent to Rooppur

Nuclear Power Plant: Elemental and multivariate statistical approach. *Applied Radiation and Isotopes,* 196**,** 110784.

SCHORR, J., THERAMPILLY, S., JIAO, L., LONGREE, P., SINGER, H. & HOLLENDER, J. 2023. Closing the gap: Ion chromatography coupled to high-resolution mass spectrometry to trace highly polar anionic substances in groundwater. *Science of The Total Environment,* 889**,** 164170.

SERA, K. 2018. Particle-Induced X-Ray Emission. *In:* THE SURFACE SCIENCE SOCIETY OF, J. (ed.) *Compendium of Surface and Interface Analysis.* Singapore: Springer Singapore.

SETIA, R., DHALIWAL, S. S., SINGH, R., SINGH, B., KUKAL, S. S. & PATERIYA, B. 2023. Ecological and human health risk assessment of metals in soils and wheat along Sutlej river (India). *Chemosphere,* 312**,** 137331.

SHARMA, M. K. & BURNETT, J. L. 2021. Sensitivity and low-energy response of the Small Anode Germanium well detector with ceramic insert. *Nuclear Instruments and Methods in Physics Research Section A: Accelerators, Spectrometers, Detectors and Associated Equipment,* 988**,** 164943.

SINGH, B. S. M., SINGH, D. & DHAL, N. K. 2022. Enhanced phytoremediation strategy for sustainable management of heavy metals and radionuclides. *Case Studies in Chemical and Environmental Engineering,* 5**,** 100176.

SINGH, P., PURAKAYASTHA, T. J., MITRA, S., BHOWMIK, A. & TSANG, D. C. W. 2020. River water irrigation with heavy metal load influences soil biological activities and risk factors. *Journal of Environmental Management,* 270**,** 110517.

SKERRATT-LOVE, K. L., GEORGE, J. L., BELL, A. M. T., SWEENEY, F., CUTFORTH, D., LONERGAN, C. E., DIXON, D. R., KRUGER, A. A. & BINGHAM, P. A. 2023. The effects of phosphorus pentoxide additions on the thermal, rheological, and structural properties of sodium borosilicate glass. *Journal of Non-Crystalline Solids,* 600**,** 121999.

SUH, M., CASTEEL, S., DUNSMORE, M., RING, C., VERWIEL, A. & PROCTOR, D. M. 2019. Bioaccessibility and relative oral bioavailability of cobalt and nickel in residential soil and dust affected by metal grinding operations. *Science of The Total Environment,* 660**,** 677-689.

SYLVIE DÉSIRÉE, N. T., ARMEL ZACHARIE, E. B., THÉRÈSE RAÏSSA, M., VINCENT LAURENT, O. & PAUL-DÉSIRÉ, N. 2021. Risk assessment of trace metals in Mefou River sediments, West-Africa. *Heliyon,* 7**,** e08606.

TARASOVA, N., ZANIN, A., SOBOLEV, P. & IVANOV, A. 2022. New approaches to the synthesis of modified red phosphorus under the high-energy radiation. *Phosphorus, Sulfur, and Silicon and the Related Elements,* 197**,** 608-609.

THOMASARRIGO, L. K. & KRETZSCHMAR, R. 2022. Iron speciation changes and mobilization of colloids during redox cycling in Fe-rich, Icelandic peat soils. *Geoderma,* 428**,** 116217.

TOMNO, R. M., NZEVE, J. K., MAILU, S. N., SHITANDA, D. & WASWA, F. 2020. Heavy metal contamination of water, soil and vegetables in urban streams in Machakos municipality, Kenya. *Scientific African,* 9**,** e00539.

TRUONG, V. M., NGUYEN, X. H., CAO, D. V., DUONG, T. T., PHAM, D. K., NGUYEN, H. P., NGUYEN, H. T., DINH, T. H., CAO, V. H., PHAN, V. C., OMER, H., SULIEMAN, A., BRADLEY, D. A. & NGUYEN, N. A. 2022. Determination of Fe and Tb concentrations in geological and environmental samples using the instrumental neutron activation analysis method combined with the $\gamma - \gamma$ coincidence technique. *Radiation Physics and Chemistry,* 200**,** 110203.

UGBEDE, F. O., OSAHON, O. D., AKPOLILE, A. F. & OLADELE, B. B. 2021. Assessment of heavy metals concentrations, soil-to-plant transfer factor and potential health risk in soil and rice samples from Ezillo rice fields in Ebonyi State, Nigeria. *Environmental Nanotechnology, Monitoring & Management,* 16**,** 100503.

UGOCHUKWU, U. C., CHUKWUONE, N., JIDERE, C., EZEUDU, B., IKPO, C. & OZOR, J. 2022. Heavy metal contamination of soil, sediment and water due to galena mining in Ebonyi State Nigeria: Economic costs of pollution based on exposure health risks. *Journal of Environmental Management,* 321**,** 115864.

UNSCEAR 2000. United Nations Scientific Committee on the Effects of Atomic Radiation: effects of Ionizing Radiation. United Nations: New York.

USEPA 1999. Federal Guidance Report No. 13: Cancer Risk Coefficients for Environmental Exposure to Radionuclides; EPA 402-R-99−001; U.S. Environmental Protection Agency: Washington, DC, USA,. *Federal Guidance Report No. 13.*

UUGWANGA, M. N. & KGABI, N. A. 2021. Heavy metal pollution index of surface and groundwater from around an abandoned mine site, Klein Aub. *Physics and Chemistry of the Earth, Parts A/B/C,* 124**,** 103067.

VAN RENSBURG, S. J., BARNARD, S. & BOOYENS, S. 2019. Comparison of phytoplankton assemblages in two differentially polluted streams in the Middle Vaal Catchment, South Africa. *South African Journal of Botany,* 125**,** 234-243.

VAN RENSBURG, S. J., BARNARD, S. & KRÜGER, M. 2016. Challenges in the potable water industry due to changes in source water quality: case study of Midvaal Water Company, South Africa. *Water SA,* 42**,** 8.

VERA, A., MORENO, J. L., GARCÍA, C., MORAIS, D. & BASTIDA, F. 2019. Boron in soil: The impacts on the biomass, composition and activity of the soil microbial community. *Science of The Total Environment,* 685**,** 564-573.

VERA, A., MORENO, J. L., SILES, J. A., LÓPEZ-MONDEJAR, R., ZHOU, Y., LI, Y., GARCÍA, C., NICOLÁS, E. & BASTIDA, F. 2021. Interactive impacts of boron and organic amendments in plant-soil microbial relationships. *Journal of Hazardous Materials,* 408**,** 124939.

VISTA, S. 2015. Use of Humic acid in agriculture.

WANG, Y., LIU, X., ZHANG, X., DAI, G., WANG, Z. & FENG, X. 2022. Evaluating wetland soil carbon stability related to iron transformation during redox oscillations. *Geoderma,* 428**,** 116222.

WEIDEMAN, E. A., PEROLD, V. & RYAN, P. G. 2019. Little evidence that dams in the Orange–Vaal River system trap floating microplastics or microfibres. *Marine Pollution Bulletin,* 149**,** 110664.

WEIDEMAN, E. A., PEROLD, V. & RYAN, P. G. 2020. Limited long-distance transport of plastic pollution by the Orange-Vaal River system, South Africa. *Science of The Total Environment,* 727**,** 138653.

WEPENER, V., VAN DYK, C., BERVOETS, L., O'BRIEN, G., COVACI, A. & CLOETE, Y. 2011. An assessment of the influence of multiple stressors on the Vaal River, South Africa. *Physics and Chemistry of the Earth, Parts A/B/C,* 36**,** 949-962.

WHO 2022. World Health Organisation: Guidelines For Drinking Water Quality. Geneva.

WILLIAMS, J. & PILLAY, A. 2011. Metals, Metalloids and Toxicity in Date Palms: Potential Environmental Impact. *Journal of Environmental Protection,* 02.

WINDE, F., BRUGGE, D., NIDECKER, A. & RUEGG, U. 2017. Uranium from Africa – An overview on past and current mining activities: Re-appraising associated risks and chances in a global context. *Journal of African Earth Sciences,* 129**,** 759-778.

WINDE, F. & DE VILLIERS, A. B. 2002. The nature and extent of uranium contamination from tailings dams in the Witwatersrand gold mining area (South Africa). *Uranium in the aquatic environment*. Springer.

WINDE, F. & VAN DER WALT, I. 2004. The significance of groundwater–stream interactions and fluctuating stream chemistry on waterborne uranium contamination of streams—a case study from a gold mining site in South Africa. *Journal of Hydrology,* 287**,** 178-196.

WOLKERSDORFER, C., MUGOVA, E., DAGA, V. S., CHARVET, P. & VITULE, J. R. S. 2021. Effects of Mining on Surface Water—Case Studies∗∗∗. *Reference Module in Earth Systems and Environmental Sciences.* Elsevier.

WORDEN, R. H. 2005. ANALYTICAL METHODS | Geochemical Analysis (Including X-ray). *In:* SELLEY, R. C., COCKS, L. R. M. & PLIMER, I. R. (eds.) *Encyclopedia of Geology*. Oxford: Elsevier.

WORLANYO, A. S. & JIANGFENG, L. 2021. Evaluating the environmental and economic impact of mining for post-mined land restoration and land-use: A review. *Journal of Environmental Management,* 279**,** 111623.

YAN, L., LE, Q. V., SONNE, C., YANG, Y., YANG, H., GU, H., MA, N. L., LAM, S. S. & PENG, W. 2021. Phytoremediation of radionuclides in soil, sediments and water. *Journal of Hazardous Materials,* 407**,** 124771.

YATES, H. S. A., CARTER, J. F., HUNGERFORD, N. L. & FLETCHER, M. T. 2023. Ion chromatography and ion chromatography / mass spectrometry as a complementary analysis technique for amino acid analysis in food, a review. *Food Chemistry Advances*, 3**,** 100415.

YOUSEFI, G., SAFADOUST, A., MAHBOUBI, A. A., GHARABAGHI, B., MOSADDEGHI, M. R., AHRENS, B. & SHIRANI, H. 2014. Bromide and lithium transport in soils under long-term cultivation of alfalfa and wheat. *Agriculture, Ecosystems & Environment,* 188**,** 221-228.

ZAKALY, H. M. H., UOSIF, M. A. M., ISSA, S. A. M., TEKIN, H. O., MADKOUR, H., TAMMAM, M., EL-TAHER, A., ALHARSHAN, G. A. & MOSTAFA, M. Y. A. 2021. An extended assessment of natural radioactivity in the sediments of the mid-region of the Egyptian Red Sea coast. *Marine Pollution Bulletin,* 171**,** 112658.

ZHANG, Q., GUILIN, H., LIU, M., ZHANG, S., WANG, L. & ZHU, G. 2022. Environmental implications of agricultural abandonment on Fe cycling: Insight from iron forms and stable isotope composition in karst soil, southwest China. *Environmental Research,* 215**,** 114377.

ZHANG, Z., ZHANG, Y., GUO, Y., CHEN, X. & CHEN, L. 2021. Impurity element analysis of aluminum hydride using PIXE, XPS and elemental analyzer technique. *Nuclear Instruments and Methods in Physics Research Section B: Beam Interactions with Materials and Atoms,* 488**,** 1-4.

ZHAO, W., BI, X., PENG, Y. & BAI, M. 2022. Research advances of the phosphorus-accumulating organisms of Candidatus Accumulibacter, Dechloromonas and Tetrasphaera: Metabolic mechanisms, applications and influencing factors. *Chemosphere,* 307**,** 135675.

ZHOU, M., LI, X., ZHANG, M., LIU, B., ZHANG, Y., GAO, Y., ULLAH, H., PENG, L., HE, A. & YU, H. 2020a. Water quality in a worldwide coal mining city: A scenario in water chemistry and health risks exploration. *Journal of Geochemical Exploration,* 213**,** 106513.

ZHOU, Q., YANG, N., LI, Y., REN, B., DING, X., BIAN, H. & YAO, X. 2020b. Total concentrations and sources of heavy metal pollution in global river and lake water bodies from 1972 to 2017. *Global Ecology and Conservation,* 22**,** e00925.

ZHU, K., KERRY, M., SERR, B. & MINTERT, M. 2023. Parts per billion of nitrite in microcrystalline cellulose by ion chromatography mass spectrometry with isotope labeled internal standard. *Journal of Pharmaceutical and Biomedical Analysis,* 235**,** 115648.

ZUPUNSKI, L., STREET, R., OSTROUMOVA, E., WINDE, F., SACHS, S., GEIPEL, G., NKOSI, V., BOUAOUN, L., HAMAN, T., SCHÜZ, J. & MATHEE, A. 2023. Environmental exposure to uranium in a population living in close proximity to gold mine tailings in South Africa. *Journal of Trace Elements in Medicine and Biology,* 77**,** 127141.

OTHER REFERENCES

Heavy metal concentrations and water quality assessment of different types of drinking water wells in the Erdenet Cu–Mo mining area. Enkhuur Munkhsuld, Takehiko Murayama, Keisuke Fukushi, Shigeo Nishikizawa, Baasansuren Gankhurel, Tserenkhand Batbold, Altansukh Ochir. *Discover Environment* (2024) **2**:12. pp 1 – 21. https://doi.org/10.1007/s44274-024-00037-1

https://www.youtube.com/watch?v=ha6x3uJVJ_Y&list=RDCMUCGAgjGCEH2SDl12M91D-10Q